A Neo-Substrate that Amplifies Catalytic Activity of Parkinson's-Disease-Related Kinase PINK1

Nicholas T. Hertz,[1,2] Amandine Berthet,[6] Martin L. Sos,[1] Kurt S. Thorn,[5] Al L. Burlingame,[4] Ken Nakamura,[3,6] and Kevan M. Shokat[1,*]

[1]Howard Hughes Medical Institute and Department of Cellular and Molecular Pharmacology
[2]Graduate Program in Chemistry and Chemical Biology
[3]Department of Neurology and Graduate Programs in Neuroscience and Biomedical Sciences
[4]Department of Pharmaceutical Chemistry
[5]Department of Biochemistry and Biophysics
University of California, San Francisco, San Francisco, CA 94158, USA
[6]Gladstone Institute of Neurological Disease, 1650 Owens Street, San Francisco, CA 94158, USA
*Correspondence: kevan.shokat@ucsf.edu
http://dx.doi.org/10.1016/j.cell.2013.07.030

SUMMARY

Mitochondria have long been implicated in the pathogenesis of Parkinson's disease (PD). Mutations in the mitochondrial kinase PINK1 that reduce kinase activity are associated with mitochondrial defects and result in an autosomal-recessive form of early-onset PD. Therapeutic approaches for enhancing the activity of PINK1 have not been considered because no allosteric regulatory sites for PINK1 are known. Here, we show that an alternative strategy, a neo-substrate approach involving the ATP analog kinetin triphosphate (KTP), can be used to increase the activity of both PD-related mutant PINK1^{G309D} and PINK1^{WT}. Moreover, we show that application of the KTP precursor kinetin to cells results in biologically significant increases in PINK1 activity, manifest as higher levels of Parkin recruitment to depolarized mitochondria, reduced mitochondrial motility in axons, and lower levels of apoptosis. Discovery of neo-substrates for kinases could provide a heretofore-unappreciated modality for regulating kinase activity.

INTRODUCTION

Parkinson's disease (PD) is characterized by the loss of dopaminergic (DA) neurons in the substantia nigra, a region in the midbrain that is critical for motor control (Lang and Lozano, 1998). Mitochondrial dysfunction has been closely linked to PD via several mechanisms (Nunnari and Suomalainen, 2012; Rugarli and Langer, 2012), including mutations in the mitochondria-specific kinase PTEN-induced kinase 1 (PINK1) (Valente et al., 2004) and the mitochondria-associated E3 ubiquitin ligase Parkin (Kitada et al., 1998). PINK1 plays an important role in repairing mitochondrial dysfunction by responding to damage at the level of individual mitochondria. In healthy mitochondria, PINK1 is rapidly degraded by the protease ParL (Meissner et al., 2011), but in the presence of inner membrane depolarization, PINK1 is stabilized on the outer membrane, where it recruits and activates Parkin (Narendra et al., 2010), blocks mitochondrial fusion and trafficking (Clark et al., 2006; Deng et al., 2008; Wang et al., 2011), and ultimately triggers mitochondrial autophagy (Geisler et al., 2010; Narendra et al., 2008; Youle and Narendra, 2011). The PINK1 pathway has also been linked to the induction of mitochondrial biogenesis and the reduction of mitochondria-induced apoptosis in neurons, the latter phenotype due at least in part to the effect of PINK1 on mitochondrial motility, a neuron-specific phenotype (Deng et al., 2005; Petit et al., 2005; Pridgeon et al., 2007; Shin et al., 2011; Wang et al., 2011).

Individuals homozygous for PINK1 loss-of-function mutations can develop a form of early-onset PD that results from highly selective DA neuronal loss and that, in at least one clinical case, shares the Lewy body pathology of sporadic PD (Gautier et al., 2008; Geisler et al., 2010; Haque et al., 2008; Henchcliffe and Beal, 2008; Petit et al., 2005; Samaranch et al., 2010). Recent work has shown that, of 17 clinically relevant PINK1 mutations, those mutants that affect catalytic activity but do not affect cleavage or subcellular localization have the most dramatic effect on neuron viability, further supporting a role for PINK1 activity in the prevention of neurodegeneration (Song et al., 2013). One of the most common of the catalytic mutants, PINK1^{G309D}, shows an ∼70% decrease in kinase activity and abrogates the neuroprotective effect of PINK1 (Petit et al., 2005; Pridgeon et al., 2007). However, lower PINK^{G309D} catalytic activity can be rescued by overexpression of PINK1^{WT}, and increasing PINK1 activity by PINK1^{WT} overexpression has been shown to reduce staurosporine- and oxidative-stress-induced apoptosis in multiple cell lines, suggesting that enhanced

PINK1 activity could be an effective therapeutic strategy for PD (Arena et al., 2013; Deng et al., 2005; Kondapalli et al., 2012; Petit et al., 2005; Pridgeon et al., 2007).

Recognizing the therapeutic potential of PINK1/Parkin pathway activation, we began investigating mechanisms for the pharmacological activation of PINK1. Small-molecule activation of kinases is typically accomplished by binding allosteric regulatory sites. For example, natural products such as phorbol esters bind to the lipid-binding domain of PKCs and recruit the kinase to the membrane (Castagna et al., 1982; Nishizuka, 1984); separately, the AMP-activated protein kinase (AMPK) is activated by binding of AMP to an allosteric site (Ferrer et al., 1985; Hardie et al., 2012). However, PINK1 contains no known small-molecule binding sites. Another potential strategy might involve manipulation of protein interaction sites or the active site, given that synthetic ligands have been identified that bind to the protein docking sites on the kinase PDK1 (Hindie et al., 2009; Wei et al., 2010) and, separately, that Src activity can be controlled by chemical complementation of an active site catalytic residue, allowing ATP to be accepted only when imidazole was provided to mutant Src (Ferrando et al., 2012; Qiao et al., 2006). However, these approaches were not applicable to PINK1 as no structural data for PINK1 are available.

We next turned our attention to sites within PINK1 known to alter its function or stability. Four PINK1 disease-associated mutations, including G309D, occur in an unusual insertion in the canonical kinase fold. Human PINK1, as well as several orthologs, share three such large (>15 amino acid [AA]) insertions in the N-terminal kinase domain (Figure S1A available online) (Cardona et al., 2011; Mills et al., 2008) that provide the majority of contacts to the adenine ring of ATP. Inserts in the active site of several enzymes have been shown to alter substrate specificity. In one example, the deubiquitinase UCH-L5 can hydrolyze larger ubiquitin chains only when a >14 AA loop is present in the active site (Zhou et al., 2012). In another example, protein engineering of alkyl guanine DNA alkyltransferase through insertion of a loop into the active site allows for recognition of an enlarged O^6-modified guanine substrate not accepted by the enzyme without the loop insertion (Heinis et al., 2006). In light of these findings, the three insertions in PINK1's adenine-binding N-terminal subdomain led us to believe that PINK1 might also exhibit altered substrate specificity.

In considering the possibility that nucleotides other than ATP could be substrates for kinases, we noticed that CK2 can utilize multiple substrates as phospho-donors—guanosine triphosphate (GTP) as well as ATP, though its activity with GTP is much lower (Niefind et al., 1999). Though it is uncommon for eukaryotic protein kinases to accept alternative substrates in the ATP binding site, kinases engineered with a single mutation to the gatekeeper residue often tolerate ATP analogs with substitutions at the N^6 position (Liu et al., 1998b; Shah et al., 1997). Importantly, no wild-type (WT) kinase we had previously studied had shown the ability to accept N^6-modified ATP analogs (Figure S1B).

We discovered that, unlike any kinase we have studied, PINK1 accepts the neo-substrate N^6 furfuryl ATP (kinetin triphosphate, KTP) with higher catalytic efficiency than its endogenous substrate, ATP. We also found that the metabolic precursor of this neo-substrate (kinetin) can be taken up by cells and converted to the nucleotide triphosphate form, which leads to accelerated Parkin recruitment to depolarized mitochondria, diminished mitochondrial motility in axons, and suppression of apoptosis in human-derived neural cells, all in a PINK1-dependent manner.

RESULTS

PINK1 Accepts N^6-Modified ATP Analog Kinetin Triphosphate

We expressed both PINK1^{WT} and PINK1^{G309D} GST-tagged kinase domains ($_{156-496}$PINK1) in *E. coli* (Figure S2A) and performed kinase assays with a series of neo-substrate analogs. As expected, PINK1^{G309D} displayed reduced activity with ATP; interestingly, however, incubation with N^6 furfuryl ATP (KTP) (Figure 1A) led to increased levels of transphosphorylation of the mitochondrial chaperone hTRAP1 (residues 60–704) (Figure 1B) and autophosphorylation with both PINK1^{G309D} and PINK1^{WT} (Figures 1C and 1D). Using a phospho-peptide capture and release strategy (Blethrow et al., 2008; Hertz et al., 2010), we were able to identify the T257 autophosphorylation site (Kondapalli et al., 2012) using KTP as the phospho-donor for PINK1 (Figure 1E), which showed that this neo-substrate is capable of supporting bona fide PINK1-dependent substrate phosphorylation.

PINK1 is intrinsically highly unstable, especially so when produced in bacteria (Beilina et al., 2005); therefore, in order to confirm the PINK1 dependency of the observed kinase activity, we took several steps to optimize PINK1 expression. We constructed several FLAG$_3$-tagged truncation variants of PINK1 and induced expression using baculovirus-infected *SF21* insect cells (Figure S2B). C-terminally tagged $_{112-581}$PINK1FLAG$_3$ expressed the most soluble protein. However, the amount was far below what we required for biochemical characterization (Figure S2C). Hypothesizing that PINK1 might require interaction with other proteins to fold properly, we coexpressed proteins known to associate with PINK1, such as DJ-1, Parkin, and TRAP1. Coexpression of full-length TRAP1 dramatically increased the stability of PINK1 (Figure S2C). This finding enabled us to express larger amounts of properly folded PINK1^{WT}, PINK1^{G309D}, and a kinase-dead PINK1^{kddd} (residues 112–581 with K219A, D362A, and D384A [Figure S1A]). In line with our initial observations, *SF21*-produced-PINK1 activity is also enhanced using KTP, but not other nucleotides (Figure 1F). We confirmed that PINK1^{kddd} has severely compromised activity (Figures 1G and S2D) and were able to show that PINK1^{WT} could autophosphorylate with a 3.9 ± 1.3-fold higher (p = 0.02; t test) V_{max} and a higher K_M (27.9 ± 4.9 μM versus 74.6 ± 13.2 μM) for the neo-substrate KTP versus ATP (Figures 1G, S2E, and S2F). As the previous assays utilized ATP with a γ-thiophosphate as a tracer, we wanted to confirm the activity using an orthogonal tracer, γ-^{32}P ATP, to visualize PINK1 activity. Therefore, we generated KTP with a γ-^{32}P-labeled phosphate and were able to see that, using this orthogonally labeled version of KTP, PINK1^{WT} transphosphorylation of $_{60-704}$TRAP1 is increased relative to γ-^{32}P ATP (Figure S2G).

Because KTP would have to compete with millimolar intracellular ATP concentrations in order to function, we
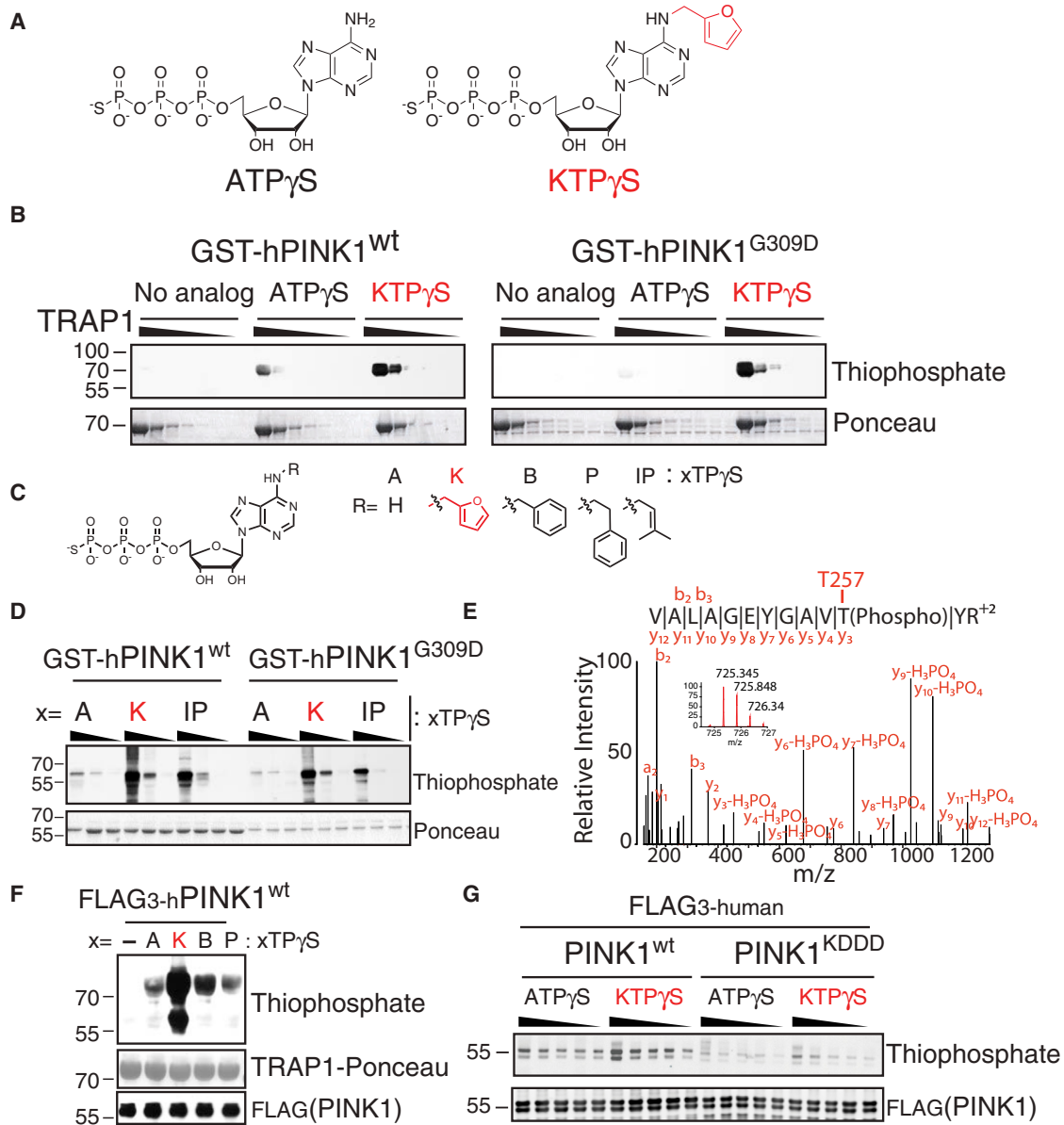
Figure 1. Neo-Substrate KTP Amplifies PINK1 Kinase Activity In Vitro

(A) Chemical structure of kinase substrate adenosine triphosphate with gamma thiophosphate (ATPγS) and neo-substrate kinetin triphosphate gamma thio-phosphate (KTPγS).

(B) PINK1 transphosphorylation kinase assay with 43 nM PINK1 and substrate $_{60-704}$TRAP1 (1 mg/ml highest concentration with 1:3 dilution across lanes) and 500 μM indicated nucleotide shown in (C); PINK1 activity was analyzed by immunoblotting for thiophospho-labeled TRAP1.

(D) PINK1 autophosphorylation kinase assay with 4.3 μM PINK1 and 100, 200, and 400 μM nucleotide (as indicated in C); PINK1 activity analyzed by immu-noblotting for thiophospho-labeled PINK1.

(E) PINK1 autophosphorylation site identified by specific peptide capture and LCMSMS found only with PINK1^{WT} and KTPγS, indicating that this nucleotide is utilized as a bona fide substrate.
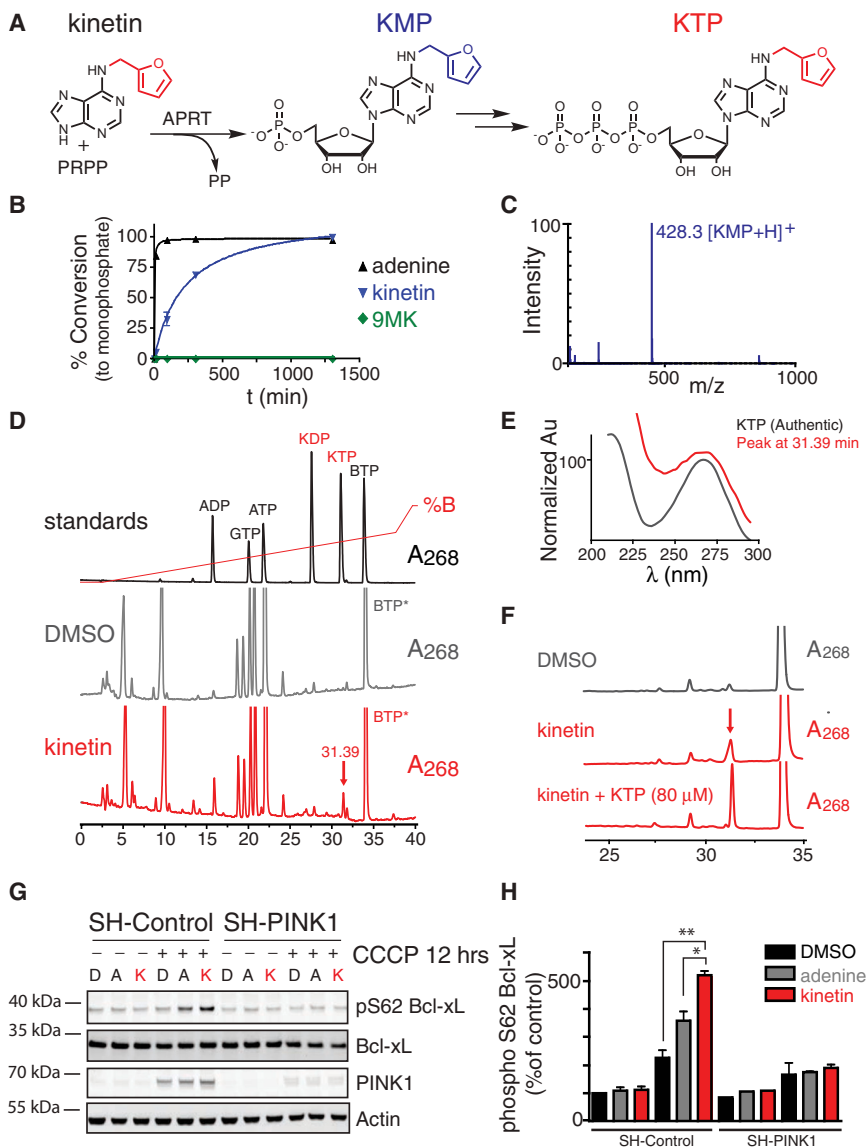
(F) *SF21*-produced PINK1 was incubated with $_{60-704}$TRAP1 and the indicated nucleotide (structure shown in C and analyzed as in B–D).

(G) PINK1 kinase assay with indicated nucleotide (250–1,250 μM in increments of 250 μM) analyzed as in (B–D) reveals much reduced phosphorylation activity with PINK1^{KDDD} (lanes 11–20); increased autophosphorylation was seen with neo-substrate KTPγS over endogenous substrate ATPγS.

See also Figures S1 and S2.

performed a competition assay with γ-thiophosphate-labeled KTP versus ATP. We found that the KTPγS signal persisted even when ATP was present at 4-fold greater concentration than KTPγS (2 mM versus 0.5 mM) (Figure S2H), suggest-ing that PINK1 can be activated by KTP in the presence of cellular ATP.

Figure 2. Neo-Substrate Precursor Kinetin Leads to KTP in Human Cells and Activates PINK1-Dependent Phosphorylation of Bcl-xL

(A) Schematic of the ribosylation reaction of kinetin to KMP via APRT and PRPP followed by cellular conversion to KTP.

(B) LCMS analysis of production of either AMP (adenine) or KMP (kinetin and 9MK) by LCMS analysis reveals that kinetin can undergo APRT mediated ribosylation to KMP, but N^9 methyl-kinetin cannot.

(C) LCMS analysis of kinetin reaction; major peak represents KMP+H peak at 428.3 mass/charge ratio (m/z).

(D) HPLC analysis of standards (ADP, GTP, ATP, KDP, KTP, and BTP), cellular lysate of DMSO, or kinetin-treated HeLa cells with 250 μM BTP* addition reveals a peak present in kinetin-treated cells at 31.39 min.

(E) Absorbance spectrum of peak at 31.39 min in kinetin-treated cells compared to absorbance spectrum of KTP in standard cells.

(F) Zoom of HPLC analysis of DMSO or kinetin-treated cell lysate with BTP addition or kinetin cell lysate with BTP addition and KTP addition reveals an increase in the peak that coelutes with KTP (186%), where BTP decreases to 76% of original area, suggesting that the peak is KTP.

(G) Immunoblot analysis with the indicated antibodies for phosphorylation on serine 62 of Bcl-xL reveals an increase following kinetin treatment.

(H) Quantitative analysis of data shown in (G) in which a significant increase in the phosphorylation of Bcl-xL on serine 62 with pretreatment with kinetin versus DMSO or adenine (p = 0.01 and p = 0.04; t test) in SH-control expressing cells not in SH-PINK1 cells. p values shown are the result of two-tailed Student's t test; *p < 0.05 and **p ≤ 0.01; all values shown are mean ± SEM.

See also Table 1 and Figure S3.

KTP Is Produced in Human Cells upon Treatment with KTP Precursor Kinetin

Our results showing in vitro increases in PINK1 activity using KTP led us to investigate the ability to achieve enhanced activity of PINK1 in cells. One major challenge to activating PINK1 in cells is that ATP analogs, like KTP, are not membrane permeable; however, previous work has shown that certain cytokinins can be taken up by human cells and converted to the nucleotide triphosphate form (Ishii et al., 2003). Additionally, recent work in cells expressing hypomorphic mutant CDK2 alleles showed that the activity of CDK2 could be increased in cells by providing nucleotide analog precursors that can be converted to the nucleotide triphosphate form and are able to fit into the hypomorphic CDK2 active site (Merrick et al., 2011).

The first step in bioconversion is ribosylation of the cytokinin to a 5′-monophosphate form, which can be mediated by adenine phospho-ribosyl transferase (APRT) (Kornberg et al., 1955; Lieberman et al., 1955b) (Figure 2A). Following established protocols (Parkin et al., 1984), we incubated adenine, kinetin, or negative control N^9 methyl-kinetin (9MK) with 5′-phosphoribosyl pyrophosphate (PRPP) and APRT and assayed the reaction by LCMS (Figure 2B). Adenine converted rapidly to AMP, achieving near-complete conversion (84%) after 10 min of reaction time; kinetin's conversion to KMP (Figures 2B and 2C) was markedly slower, requiring 150 min for half to be converted. The control compound 9MK is not converted to KMP even after 16 hr of incubation (Figure 2B), whereas kinetin was completely converted to KMP in this time frame. This experiment demonstrated that the ribosylation of kinetin is biosynthetically possible using the enzymatic route for AMP production.

Our next step was to ask whether KMP could be converted to the nucleotide triphosphate form (KTP) required for it to

	Concentration
ATP	$1,950 \pm 421$ μM
KTP	68 ± 13.3 μM

See also Figures 2 and S3.

serve as a neo-substrate for PINK1. Work by many labs has demonstrated that ribosyl nucleotide analogs can be phosphorylated to nucleotide triphosphate forms by endogenous enzymes (Krishnan et al., 2002; Lieberman et al., 1955a; Ray et al., 2004). To confirm the presence of intracellular KTP following incubation with kinetin, we adapted an ion-pairing HPLC analysis method on a reverse-phase C18 column (Figure 2D) according to established methods (Vela et al., 2007). After treatment with kinetin or DMSO, cells were lysed and analyzed for the presence of peaks eluting at the retention time of KTP. An internal standard of BTP (denoted by an asterisk in Figures 2D, 2F, S3A, and S3B) was added following lysis. Analysis of the kinetin-treated cells revealed a peak that coelutes (offset by a consistent amount [Figure S3A]) with synthetic KTP, a result not seen in any of our controls (Figures 2D, S3A, and S3B). The UV absorbance maximum measured with a diode array detector is the same as KTP (Figure 2E) (absorbance peak at 268 nm) and is significantly different than that of either ATP or GTP (Figure S3C), both of which have significantly different retention times. In a separate HPLC analytical run, an aliquot of authentic KTP (to 80 μM) was added to authenticate the putative KTP peak (Figure 2F). The peak grew to 186% of its original area, whereas the peak of the standard BTP decreased to 76% of its original area, suggesting that these were the same substance. From these data, we calculate that an ATP concentration of $1,950 \pm 421$ μM and a KTP concentration of 68 ± 13 μM (three biological replicates, Table 1) are produced upon incubation with kinetin.

Kinetin Increases Phosphorylation of PINK1 Substrate Antiapoptotic Protein Bcl-xL

Bcl-xL is a member of the Bcl-2 protein family that plays a key regulatory role in mitochondrial-induced apoptosis (Adams and Cory, 1998; Gross et al., 1999). PINK1 phosphorylates Bcl-xL at serine 62 in response to mitochondrial depolarization blocking cleavage to a proapoptotic form (Arena et al., 2013). We therefore measured PINK1-dependent phosphorylation of Bcl-xL in human SH-SY5Y cells following carbonyl cyanide *m*-chlorophenyl hydrazone (CCCP)-induced depolarization. We analyzed DMSO, 50 μM adenine, or 50 μM kinetin-treated SH-SY5Y cells at 12 hr after 50 μM CCCP addition (Figure 2G) and observed a significant ($p = 0.01$ and $p = 0.04$; t test) (Figures 2G and 2H) increase in phospho-Bcl-xL (S62) only in kinetin-treated cells compared to DMSO or adenine, where PINK1 expression has not been silenced by small hairpin RNA (shRNA). These results confirm that CCCP-mediated depolarization will induce PINK1-dependent phosphorylation on S62 and suggest that kinetin stimulates this activity in a PINK1-dependent manner.

Kinetin Accelerates Parkin Recruitment to Depolarized Mitochondria in a PINK1-Dependent Manner

Parkin recruitment to depolarized mitochondria is PINK1 dependent (Narendra et al., 2010); therefore, we postulated that enhancement of PINK1 activity might accelerate this process. We treated cells with either kinetin or adenine (Figure 3A) and measured Parkin localization following CCCP-mediated mitochondria depolarization. HeLa cells, which have low levels of endogenous PINK1 and PARKIN, were transfected with PINK1[WT] or PINK1[G309D], mCherryParkin, and mitochondrial-targeted GFP (mitoGFP). After 48 hr of incubation with 25 μM adenine, kinetin, or equivalent DMSO (Figure 3B), we imaged every 5 min following CCCP-mediated depolarization of mitochondria (Figures 3C, 3D, and S4A–S4F) and calculated the percentage of GFP-labeled mitochondria with mCherryParkin associated (Figures 3E and 3F and Table 2).

In line with previous reports (Narendra et al., 2010), transfection of PINK1[G309D] slowed the 50% recruitment (R_{50}) time of mCherryParkin to depolarized mitochondria (23 ± 2 min versus 15 ± 1 min R_{50}) (Figure 3E and Table 2). The addition of kinetin, but not adenine, decreased the R_{50} for Parkin in PINK1[G309D] cells from 23 ± 2 min to 15 ± 2 min and also decreased the R_{50} for PINK1[WT] cells from 15 ± 1 min to 10 ± 2 min (Figures 3E and 3F and Table 2). Using an image analysis algorithm (Figures S4G and S4H) that quantified the time-dependent change in colocalization, we found that PINK1[WT]-expressing cells achieved a maximum change in colocalization of 0.112 with DMSO or adenine and 0.13 with kinetin treatment (Figure S4I). PINK1[G309D]-expressing cells treated with DMSO or adenine achieved a change in colocalization of 0.076, but upon addition of kinetin, they returned to near-PINK1[WT] levels (0.124) (Figure S4J). These results suggested significant rescue of PINK1[G309D] activity using kinetin. Two-way ANOVA analysis revealed that kinetin has an effect in both cases (WT, $F = 24.10$ and $p < 0.0001$; G309D, $F = 54.14$ and $p < 0.0001$). Additionally, in line with in vitro results in which benzyl triphosphate (BTP) did not activate PINK1 as robustly as KTP (Figure 1F), benzyl adenine is in general less active than kinetin in cells, although it also demonstrated some acceleration of Parkin recruitment (data not shown). However, benzyl adenine has been shown to be cytotoxic in other assays (Ishii et al., 2002); therefore, despite PINK1 activation potential of benzyl adenine, we decided to focus on KTP to use as a neo-substrate to amplify PINK1 activity.

To test the PINK1 dependency of our findings, we assayed PINK1 activity by using phospho-specific antibodies raised against the PINK1-specific S65 phospho-site on Parkin (Kondapalli et al., 2012). We observed a small but reproducible increase in the phosphorylation level of Parkin following CCCP treatment in a PINK1-dependent manner (Figures S5A and S5B). In a finding that supported our colocalization results, we also found that the addition of neo-substrate kinetin ($p = 0.03$; t test), but not adenine ($p = 0.30$; t test), to PINK1[G309D] mutant-expressing cells increased the phosphorylation levels of Parkin (Figures S5C and S5D). The addition of an adenosine kinase inhibitor (AKI) blocking the conversion of kinetin to KTP prevented this effect ($p = 0.31$; t test) (Figure S5D).
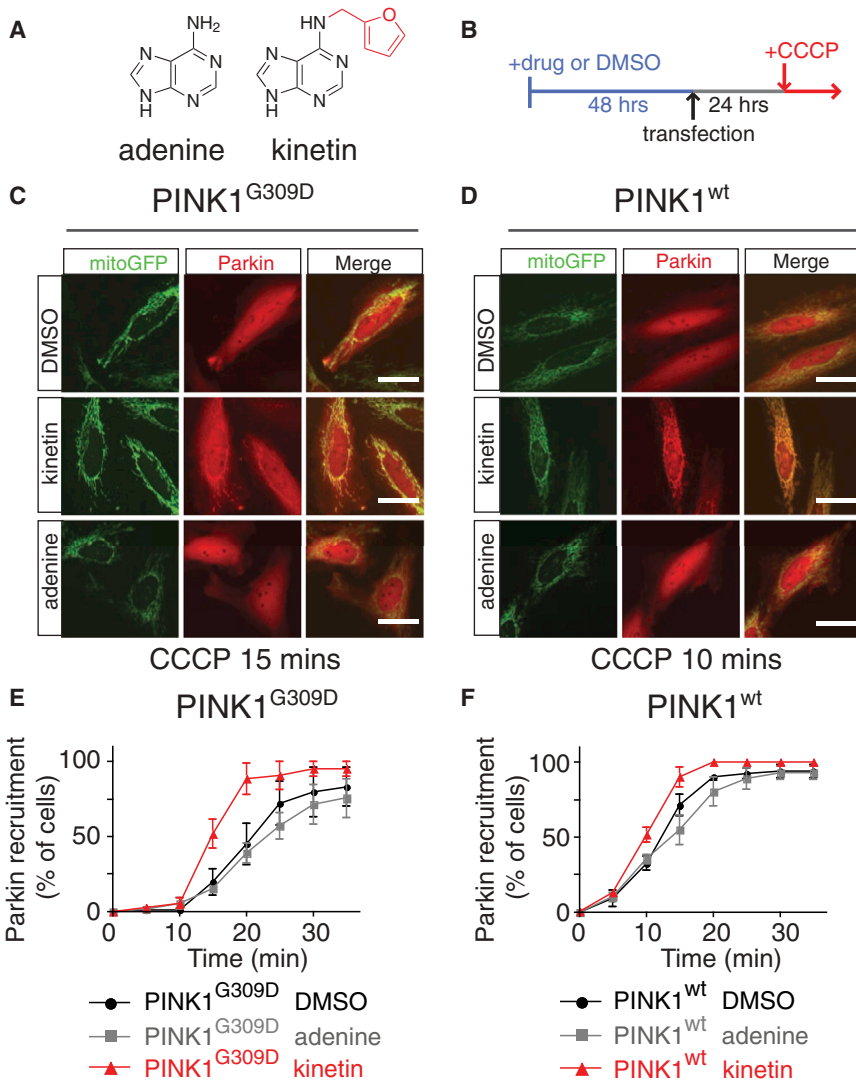
Figure 3. PINK1 Neo-Substrate Kinetin Accelerates PINK1-Dependent Parkin Recruitment in Cells

(A) Chemical structure of adenine or kinase neo-substrate precursor kinetin.

(B) Schematic depicting HeLa cell drug treatment.

(C and D) HeLa cells treated with indicated drug and cotransfected with mitoGFP, mCherryParkin, and indicated PINK1 construct imaged at either 10 or 15 min after 5 μM CCCP addition.

(E and F) Kinetin-treated cells reached R_{50} significantly faster than with adenine or DMSO (all data shown are mean ± SEM) by two-way ANOVA analysis; kinetin has an effect in both cases when compared to adenine (WT, F = 25.41 and p < 0.0001; G309D, F = 31.89 and p < 0.0001) and DMSO (WT; F = 21.94 p < 0.0001, G309D; F = 12.79, p < 0.0011). There was no significant difference for DMSO adenine in either case (at least 150 cells/experiment; n = 3 experiments; all values are mean ± SEM).

See also Table 2 and Figure S4.

Kinetin Blocks Mitochondrial Motility in Axons in a PINK1-Dependent Manner

Increasing PINK1 activity markedly decreases the mobility of axonal mitochondria, and this is thought to be the first step in the sequestration and removal of damaged mitochondria (Wang et al., 2011). To determine whether PINK1 activation by kinetin also decreases mitochondrial motility, we examined the mobility of axonal mitochondria in rat hippocampal neurons cotransfected with mitoGFP to identify mitochondria and N-terminal mCherry-tagged synaptophysin to identify axons (Hua et al., 2011; Nakamura et al., 2011). Cells were pretreated for 48 hr with 50 μM kinetin, adenine, 9-methyl-kinetin (9MK, shown in Figure 4A), or equivalent DMSO, and mitochondrial motility was imaged live. Kymographs were generated (Figures 4B–4E) using standard techniques. Kinetin markedly inhibited the percentage of moving mitochondria when compared to DMSO (p = 0.0005; t test) (Figures 4D and 4F). In contrast, kinetin analog 9-methyl-kinetin (9MK) (Figures 4A, 4E, and 4F), which cannot be converted to a nucleotide triphosphate form, did not affect

mitochondrial motility when compared to DMSO (p = 0.86; t test). Kinetin also produced a small decrease in the velocity of mitochondria that remain in motion (p = 0.03; t test) (Figure 4G).

To confirm that kinetin decreases mitochondrial motility through effects on PINK1, we also performed experiments in hippocampal neurons derived from WT (C57BL/6) and PINK1 KO mice (Xiong et al., 2009) after treatment with DMSO, kinetin, or 9MK. Consistent with the results in rat neurons, kinetin also significantly decreased mitochondrial motility in control neurons (p < 0.0001; t test) when compared with either 9MK or DMSO (Figures 4H and S5E). However, kinetin had no effect on the motility of mitochondria in PINK1 KO neurons (Figure 4H) (p = 0.64; t test), and unlike rat-derived neurons, kinetin had no effect on the velocity of mitochondria that remain in motion (Figure 4I). These data suggest that kinetin can block mitochondrial motility in a PINK1-dependent manner and that the metabolism of kinetin to KTP is a necessary precursor for that effect.

Kinetin Decreases Apoptosis Induced by Oxidative Stress in Human-Derived Neuronal Cells in a PINK1-Dependent Manner

Previous studies have shown that PINK1 expression can block apoptosis in response to proteosomal stress induced by the proteosome inhibitor MG132 (Klinkenberg et al., 2010; Wang et al., 2007). Caspase 3/7 activity is an early marker for apoptosis. Therefore, to assess the ability of kinetin to amplify PINK1 activity to block apoptosis, we measured caspase 3/7 activity using a luminescence-based caspase 3/7 peptide cleavage assay in HeLa cells. We treated HeLa cells transfected with Parkin with

	DMSO	Adenine	Kinetin
PINK1[WT]	14 ± 1 min	15 ± 1 min	10 ± 2 min
PINK1[G309D]	20 ± 2 min	23 ± 2 min	15 ± 2 min

See also Figures 3 and S4.

DMSO or 25 μM adenine or kinetin for 48 hr, followed by 1 μM MG132 for 12 hr. We found that kinetin significantly (p = 0.005 and p = 0.004; t test) reduced caspase 3/7 cleavage versus DMSO or adenine pretreatment and that knockdown of PINK1 abrogated this effect (Figures 5A and S6A).

We then tested whether kinetin would be tolerated by cultured DA neurons. Previous work has shown KTP precursor kinetin to be extremely well tolerated in both mouse models and in human clinical testing (Axelrod et al., 2011; Shetty et al., 2011). To confirm these results, we treated DA neurons with 50 μM kinetin or adenine and measured cell density after 10 days. Kinetin and adenine have no effect on cell density, indicating that neither promotes apoptosis of cultured DA neurons (Figure S6B).

We next utilized patient-derived neuroblastoma SH-SY5Y cells, which are also known to exhibit decreased apoptosis upon overexpression of PINK1 (Deng et al., 2005; Klinkenberg

et al., 2010). We performed a dose-response assay in which SH-SY5Y cells were treated with increasing concentrations of kinetin, adenine, or DMSO for 96 hr and 1 μM MG132 for 16 hr, followed by analysis for caspase 3/7 cleavage activity. As in HeLa cells, kinetin pretreatment significantly decreased caspase 3/7 cleavage in SH-SY5Y cells (Figure 5B). Two-way ANOVA analysis revealed that kinetin has an effect when compared to DMSO or adenine (Figure 5B) (DMSO, F = 34.95 and p < 0.0001; adenine, F = 38.37 and p < 0.0001) only in cells in which we did not silence PINK1 expression via stable shRNA expression (DMSO, F = 3.552 and p = 0.084; adenine, F = 1.7 and p = 0.215) (Figures 5B, S6C, and S6D) despite a small visible effect, probably due to incomplete knockdown of PINK1 (Figure S6C). These experiments suggest that the kinetin-induced reduction in caspase 3/7 cleavage activity is PINK1 dependent.

To assay later stages of apoptosis in SH-SY5Y cells, we utilized an independent fluorescence-activated cell sorting (FACS)-based method to measure cellular apoptosis. In addition to proteosomal stress, PINK1 overexpression is known to block apoptosis induced by H_2O_2 treatment (Deng et al., 2005; Gautier et al., 2008; Petit et al., 2005; Pridgeon et al., 2007). SH-SY5Y cells were treated with 50 μM kinetin, adenine, or DMSO for 96 hr, followed by 400 μM H_2O_2 treatment for 24 hr. Using a cytometry-based FACS assay utilizing annexin V and propidium iodide staining, we determined the percentage of apoptotic cells after treatment with DMSO, adenine, or
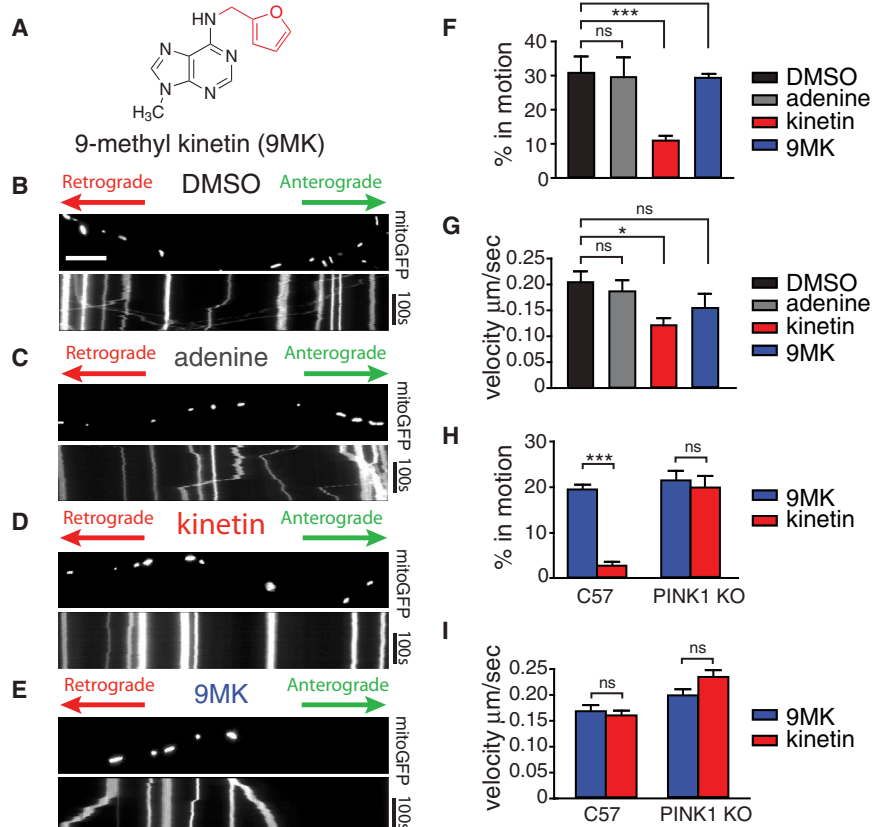
Figure 4. Kinetin Halts Axonal Mitochondrial Motility in a PINK1-Dependent Manner

(A) Chemical structure of negative control nonmetabolizable kinetin analog 9-methyl-kinetin.

(B–E) Kymograph for analysis of mitochondrial movement in representative PINK1[WT]-expressing rat-derived hippocampal axons transfected with mitoGFP. Scale bar, 10 μm.

(F) The percentage of time each mitochondrion was in motion was determined and averaged. Kinetin significantly blocks mitochondrial motility, whereas 9MK has no effect (DMSO-kinetin, p = 0.0005; DMSO-9MK, p = 0.86).

(G) Kinetin induces a small decrease in velocity (DMSO-kinetin, p = 0.03; DMSO-9MK, p = 0.24).

(H) Kymograph for analysis of mitochondrial movement in C57BL/6 shows a response to kinetin (kinetin 9MK, p < 0.0001), whereas in PINK1-knockout-derived hippocampal axons, kinetin has no effect (kinetin 9MK, p = 0.64).

(I) Both kinetin and 9MK have no effect on mitochondrial velocity of moving mitochondrion (C57BL/6 kinetin-9MK, p = 0.64; PINK1 KO, p = 0.074) (all values are mean ± SEM, analysis was two-tailed Student's t test).

See also Figure S5.
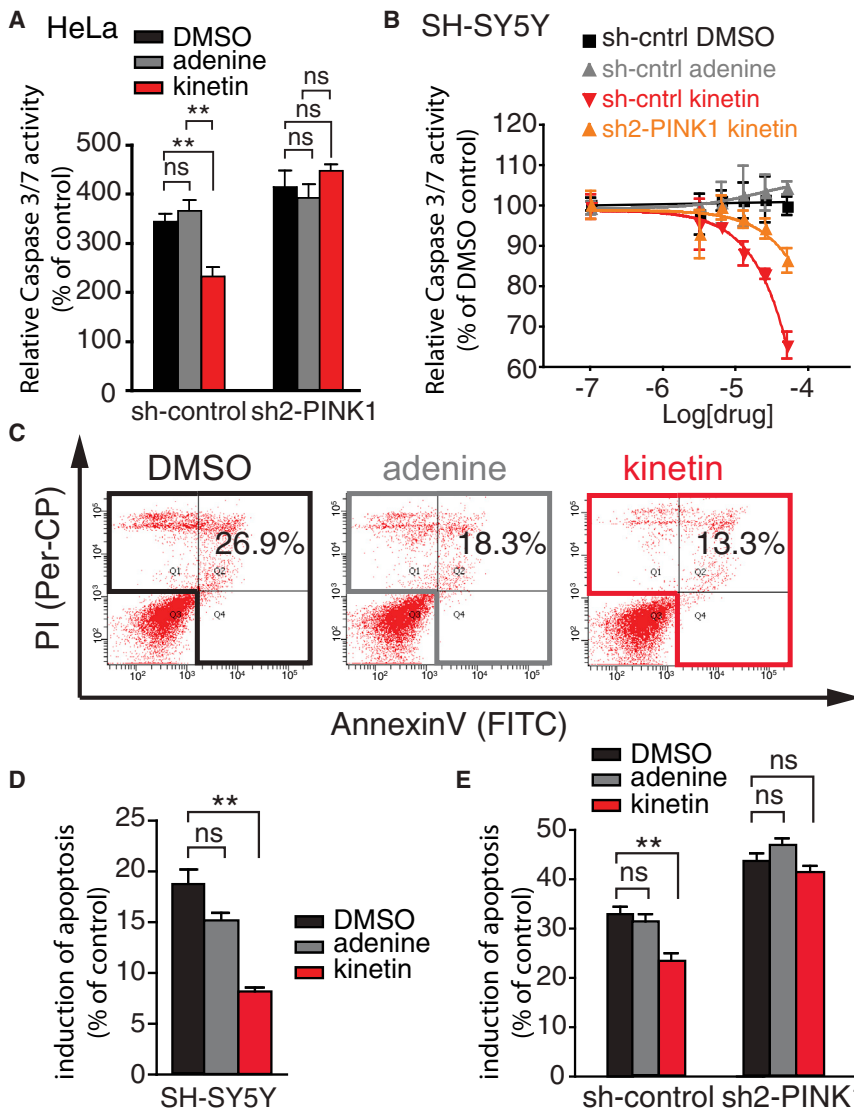
Figure 5. Kinetin Inhibits Oxidative Stress-Induced Apoptosis in Human Cells in a PINK1-Dependent Manner

(A) Caspase 3/7 cleavage activity assay following pretreatment with DMSO, adenine, or kinetin for 48 hr followed by MG132 treatment for 12 hr compared to no MG132-treated cells reveals reduced caspase 3/7 activity (p = 0.005 and p = 0.004; t test) only in sh-control-expressing cells and not in cells expressing shRNA against PINK1.

(B) Caspase 3/7 cleavage activity of SH-SY5Y cells pretreated with indicated concentration of adenine or kinetin for 96 hr followed by MG132 treatment for 12 hr in all conditions. Two-way ANOVA analysis revealed that kinetin has an effect when compared to DMSO or adenine (Figure 5B) (DMSO, F = 34.95 and p < 0.0001; adenine, F = 38.37 and p < 0.0001) but has no statistically significant effect (DMSO, F = 3.552 and p = 0.084; adenine, F = 1.7 and p = 0.215) in cells expressing an shRNA against PINK1.

(C) SH-SY5Y cells pretreated as above were stained with FITC conjugated Annexin V and propidium iodide and were analyzed by FACS.

(D) Quantification of (C) shows that kinetin-treated cells have significantly lower induction of apoptosis (DMSO-kinetin, p = 0.0023), but adenine had no effect (DMSO-adenine, p = 0.09).

(E) Indicated SH-SY5Y cell lines were treated as in (A). Kinetin-treated cells had significantly lower induction of apoptosis only when PINK1 was present (normalized to DMSO control untreated cells; sh-control DMSO-kinetin, p = 0.008; sh-PINK1 DMSO-kinetin, p = 0.23; sh-control DMSO-adenine, p = 0.48; sh-PINK1 DMSO-adenine, p = 0.23; all values are mean ± SEM; analysis was Wilcoxon t test).

See also Figure S6.

kinetin (Figure 5C). We observed a significant decrease in the total amount of apoptotic cells following kinetin treatment (Figure 5D) (DMSO versus kinetin, p = 0.0023; Wilcoxon T test) but no significant change with adenine (DMSO versus adenine, p = 0.09; Wilcoxon T test). Additionally, we observed a significant drop in apoptosis in shRNA control lentivirus-infected cells (DMSO versus kinetin, p = 0.008; Wilcoxon T test) but no kinetin effect with infection of a lentivirus expressing PINK1-silencing shRNA (Figures 5E and S6C) (DMSO versus kinetin, p = 0.23; Wilcoxon T test). These results demonstrate a PINK1-dependent antiapoptotic effect and suggest that kinetin can activate PINK1 to block oxidative stress-induced apoptosis of human neural cells.

DISCUSSION

Our investigation of a neo-substrate approach to modulating PINK1 activity has yielded three significant findings: (1) that the

ATP analog KTP can be used by both PINK1^{WT} and PINK1^{G309D}; (2) that KTP enhances both PINK1^{WT} and PINK1^{G309D} activity in vitro and in cells and, in the case of the latter version, returns it to near-WT catalytic efficiency; and (3) that KTP precursor kinetin can be applied to neurons to enhance PINK1 activity in several biologically relevant paradigms.

The finding that kinetin (or its nucleotide triphosphate form, KTP) can restore PINK1^{G309D} catalytic activity to near-WT levels in vitro and in cells, in light of the fact that mutations in PINK1 produce PD in humans, raises the possibility that kinetin may be used to treat patients who have mutant PINK1. Further, because kinetin has already been shown to be well tolerated in human trials (for familial dysautonomia, an unrelated splicing disorder) and because previous work in mice has shown that kinetin can cross the blood-brain barrier and achieve pharmacologically significant concentrations (Axelrod et al., 2011; Shetty et al., 2011), these results have the potential for near-term clinical relevance.

Although mutations in PINK1 are a rare cause of PD, the development of an effective disease-modifying therapy for

any neurodegenerative disease would be a tremendous advance and could provide important therapeutic insights into disease-modifying strategies for other types of PD. In fact, the finding that increasing PINK1 activity beyond endogenous levels can protect against a variety of apoptotic stressors (Klinkenberg et al., 2010; Petit et al., 2005; Pridgeon et al., 2007) and that kinetin can also reproduce this protection by enhancing endogenous PINK1 function raises the possibility that enhancing PINK1 activity may also have therapeutic potential for idiopathic PD.

Current kinase-targeted drugs are striking for the single modality of regulating kinase function—inhibition. However, a wide range of kinase dysregulation in disease is caused by a lack of kinase activity: desensitization of insulin receptor kinase in diabetes (Kulkarni et al., 1999); inactivation of the death-associated protein kinase (DAPK) in cancer (Kissil et al., 1997); inactivation of the LKB1 tumor-suppressor kinase in cancer (Gao et al., 2011); and decreased PINK1 activity in early-onset Parkinson's disease. Although many examples of inactive kinases causing disease have been uncovered, there have been no therapeutic approaches for enhancing kinase activity using alternative substrates. Our insights into the potential for manipulating kinase-dependent cellular processes via a specifically targeted neo-substrate may presage the ability to treat other diseases resulting from kinase misregulation with an innovative class of neo-substrate kinase activators.

EXPERIMENTAL PROCEDURES

Detailed methods for dopamine neuron cultures, PINK1 shRNA lentivirus production, and apoptosis assays can be found in the Extended Experimental Procedures.

Western Blot Analysis

Western blot analysis was carried out as described (Ultanir et al., 2012) with the indicated antibodies. See Extended Experimental Procedures for details.

Expression, Purification, and Enzymatic Characterization of PINK1

H. sapiens PINK1 kinase domain (PINK1, residues 156–496; all plasmids obtained from Addgene) with an N-terminal GST tag was expressed using a pGEX vector using standard techniques. *H. sapiens* PINK1 kinase domain with C-terminal extension (PINK1, residues 112–581) with a C-terminal $FLAG_3$ tag was coexpressed with full-length *H. sapiens* TRAP1 in the baculovirus/*Sf21* insect cell system. Following lysis, $PINK1_{112-581}$ kinase was purified using magnetic M2 FLAG affinity resin (Sigma), and the kinase reaction was performed on beads after no more than 2 hr following lysis. The reaction was performed using 50 mM Tris-HCl, 150 mM NaCl, 10 mM $MgCl_2$, 3 mM $MnCl_2$, 0.5 mM DTT, and 1 mg/ml substrate if not otherwise indicated. After reaction at room temperature with rotation, the kinase reaction was quenched with 50 mM EDTA and reacted with 1.5 mM p-nitrobenzylmesylate (PNBM) and identified by immunoblot with anti-thiophosphate ester antibody (Epitomics) (Allen et al., 2007).

Identification of PINK1 Autophosphorylation Site by Liquid Chromatography-Tandem Mass Spectrometry

Protocol was carried out as described (Ultanir et al., 2012). See Extended Experimental Procedures for details.

Enzymatic Production of KMP In Vitro

Reactions with APRT and PRPP and adenine, kinetin, or 9MK were carried out as described (Parkin et al., 1984). See Extended Experimental Procedures for details.

HPLC Analysis for KTP Production in Cells

HeLa cells were incubated with the indicated drug for 96 hr, and nucleotides were extracted and analyzed as described (Ray et al., 2004; Vela et al., 2007). See Extended Experimental Procedures for details.

Parkin Mitochondrial Translocation Assay

HeLa cells were grown in DMEM supplemented with 10% FBS. Log phase cells were plated in 24 well plates with glass coverslips (Mattek) pretreated with fibronectin. Cells were pretreated with 25 μM of the indicated compound, followed by transfection with MitoGFP, mCherryParkin, and full-length $PINK1FLAG_3$ in a 1:4:2 ratio using Fugene 6 (Promega). Fields of cells were selected by expression of MitoGFP (six fields/well, three wells/condition) and imaged at 5 min intervals following depolarization with 5 μM CCCP. Quantification was performed according to published protocols (Narendra et al., 2010) and by implementing a Matlab-based script (see Data S1).

Mitochondrial Motility Assay

All experiments were carried out according to IACUC guidelines, and UCSF IACUC approved all experiments before execution. Primary hippocampal cultures were prepared from early postnatal (P0 to P1) rat or mouse (C57BL6 or $Pink1^{-/-}$) pups, cotransfected by electroporation (Amaxa) with mitochondrial-targeted GFP (mitoGFP) to visualize mitochondria, and mCherry fused to synaptophysin (mCherrySynaptophysin) to visualize axons. Cells were pretreated for 48 hr with 50 μM kinetin, adenine, 9-methyl-kinetin, or equivalent DMSO at day 9 and imaged live in Tyrode's medium (in mM: 127 NaCl, 10 HEPES-NaOH (pH 7.4), 30 glucose, 2.5 KCl, 2 $CaCl2$, and 2 $MgCl2$) with a 60× water immersion objective on a Nikon Ti-E inverted microscope. Images were captured every 2 s for a total of 200 s, and kymographs were generated from each live-imaging movie with Metamorph software (version 7.7.3.0). Mitochondria were considered moving if they traveled more than 0.67 μm during the 200 s imaging.

SUPPLEMENTAL INFORMATION

Supplemental Information includes Extended Experimental Procedures, six figures, and one data file and can be found with this article online at http://dx.doi.org/10.1016/j.cell.2013.07.030.

REFERENCES

Adams, J.M., and Cory, S. (1998). The Bcl-2 protein family: arbiters of cell survival. Science 281, 1322–1326.

Allen, J.J., Li, M., Brinkworth, C.S., Paulson, J.L., Wang, D., Hübner, A., Chou, W.H., Davis, R.J., Burlingame, A.L., Messing, R.O., et al. (2007). A semisynthetic epitope for kinase substrates. Nat. Methods 4, 511–516.

Arena, G., Gelmetti, V., Torosantucci, L., Vignone, D., Lamorte, G., De Rosa, P., Cilia, E., Jonas, E.A., and Valente, E.M. (2013). PINK1 protects against cell death induced by mitochondrial depolarization, by phosphorylating Bcl-xL and impairing its pro-apoptotic cleavage. Cell Death Differ. 20, 920–930.

Axelrod, F.B., Liebes, L., Gold-Von Simson, G., Mendoza, S., Mull, J., Leyne, M., Norcliffe-Kaufmann, L., Kaufmann, H., and Slaugenhaupt, S.A. (2011). Kinetin improves IKBKAP mRNA splicing in patients with familial dysautonomia. Pediatr. Res. 70, 480–483.

Beilina, A., Van Der Brug, M., Ahmad, R., Kesavapany, S., Miller, D.W., Petsko, G.A., and Cookson, M.R. (2005). Mutations in PTEN-induced putative kinase 1 associated with recessive parkinsonism have differential effects on protein stability. Proc. Natl. Acad. Sci. USA 102, 5703–5708.

Blethrow, J.D., Glavy, J.S., Morgan, D.O., and Shokat, K.M. (2008). Covalent capture of kinase-specific phosphopeptides reveals Cdk1-cyclin B substrates. Proc. Natl. Acad. Sci. USA 105, 1442–1447.

Cardona, F., Sánchez-Mut, J.V., Dopazo, H., and Pérez-Tur, J. (2011). Phylogenetic and in silico structural analysis of the Parkinson disease-related kinase PINK1. Hum. Mutat. 32, 369–378.

Castagna, M., Takai, Y., Kaibuchi, K., Sano, K., Kikkawa, U., and Nishizuka, Y. (1982). Direct activation of calcium-activated, phospholipid-dependent protein kinase by tumor-promoting phorbol esters. J. Biol. Chem. 257, 7847–7851.

Clark, I.E., Dodson, M.W., Jiang, C., Cao, J.H., Huh, J.R., Seol, J.H., Yoo, S.J., Hay, B.A., and Guo, M. (2006). Drosophila pink1 is required for mitochondrial function and interacts genetically with parkin. Nature 441, 1162–1166.

Deng, H., Jankovic, J., Guo, Y., Xie, W., and Le, W. (2005). Small interfering RNA targeting the PINK1 induces apoptosis in dopaminergic cells SH-SY5Y. Biochem. Biophys. Res. Commun. 337, 1133–1138.

Deng, H., Dodson, M.W., Huang, H., and Guo, M. (2008). The Parkinson's disease genes pink1 and parkin promote mitochondrial fission and/or inhibit fusion in Drosophila. Proc. Natl. Acad. Sci. USA 105, 14503–14508.

Ferrando, I.M., Chaerkady, R., Zhong, J., Molina, H., Jacob, H.K., Herbst-Robinson, K., Dancy, B.M., Katju, V., Bose, R., Zhang, J., et al. (2012). Identification of targets of c-Src tyrosine kinase by chemical complementation and phosphoproteomics. Mol. Cell. Proteomics 11, 355–369.

Ferrer, A., Caelles, C., Massot, N., and Hegardt, F.G. (1985). Activation of rat liver cytosolic 3-hydroxy-3-methylglutaryl coenzyme A reductase kinase by adenosine 5′-monophosphate. Biochem. Biophys. Res. Commun. 132, 497–504.

Gao, Y., Ge, G., and Ji, H. (2011). LKB1 in lung cancerigenesis: a serine/threonine kinase as tumor suppressor. Protein Cell 2, 99–107.

Gautier, C.A., Kitada, T., and Shen, J. (2008). Loss of PINK1 causes mitochondrial functional defects and increased sensitivity to oxidative stress. Proc. Natl. Acad. Sci. USA 105, 11364–11369.

Geisler, S., Holmström, K.M., Treis, A., Skujat, D., Weber, S.S., Fiesel, F.C., Kahle, P.J., and Springer, W. (2010). The PINK1/Parkin-mediated mitophagy is compromised by PD-associated mutations. Autophagy 6, 871–878.

Gross, A., McDonnell, J.M., and Korsmeyer, S.J. (1999). BCL-2 family members and the mitochondria in apoptosis. Genes Dev. 13, 1899–1911.

Haque, M.E., Thomas, K.J., D'Souza, C., Callaghan, S., Kitada, T., Slack, R.S., Fraser, P., Cookson, M.R., Tandon, A., and Park, D.S. (2008). Cytoplasmic Pink1 activity protects neurons from dopaminergic neurotoxin MPTP. Proc. Natl. Acad. Sci. USA 105, 1716–1721.

Hardie, D.G., Ross, F.A., and Hawley, S.A. (2012). AMPK: a nutrient and energy sensor that maintains energy homeostasis. Nat. Rev. Mol. Cell Biol. 13, 251–262.

Heinis, C., Schmitt, S., Kindermann, M., Godin, G., and Johnsson, K. (2006). Evolving the substrate specificity of O6-alkylguanine-DNA alkyltransferase through loop insertion for applications in molecular imaging. ACS Chem. Biol. 1, 575–584.

Henchcliffe, C., and Beal, M.F. (2008). Mitochondrial biology and oxidative stress in Parkinson disease pathogenesis. Nat. Clin. Pract. Neurol. 4, 600–609.

Hertz, N.T., Wang, B.T., Allen, J.J., Zhang, C., Dar, A.C., Burlingame, A.L., and Shokat, K.M. (2010). Chemical genetic approach for kinase-substrate mapping by covalent capture of thiophosphopeptides and analysis by mass spectrometry. Curr. Protoc. Chem. Biol. 2, 15–36.

Hindie, V., Stroba, A., Zhang, H., Lopez-Garcia, L.A., Idrissova, L., Zeuzem, S., Hirschberg, D., Schaeffer, F., Jørgensen, T.J., Engel, M., et al. (2009). Structure and allosteric effects of low-molecular-weight activators on the protein kinase PDK1. Nat. Chem. Biol. 5, 758–764.

Hua, Z., Leal-Ortiz, S., Foss, S.M., Waites, C.L., Garner, C.C., Voglmaier, S.M., and Edwards, R.H. (2011). v-SNARE composition distinguishes synaptic vesicle pools. Neuron 71, 474–487.

Ishii, Y., Hori, Y., Sakai, S., and Honma, Y. (2002). Control of differentiation and apoptosis of human myeloid leukemia cells by cytokinins and cytokinin nucleosides, plant redifferentiation-inducing hormones. Cell Growth Differ. 13, 19–26.

Ishii, Y., Sakai, S., and Honma, Y. (2003). Cytokinin-induced differentiation of human myeloid leukemia HL-60 cells is associated with the formation of nucleotides, but not with incorporation into DNA or RNA. Biochim. Biophys. Acta 1643, 11–24.

Kissil, J.L., Feinstein, E., Cohen, O., Jones, P.A., Tsai, Y.C., Knowles, M.A., Eydmann, M.E., and Kimchi, A. (1997). DAP-kinase loss of expression in various carcinoma and B-cell lymphoma cell lines: possible implications for role as tumor suppressor gene. Oncogene 15, 403–407.

Kitada, T., Asakawa, S., Hattori, N., Matsumine, H., Yamamura, Y., Minoshima, S., Yokochi, M., Mizuno, Y., and Shimizu, N. (1998). Mutations in the parkin gene cause autosomal recessive juvenile parkinsonism. Nature 392, 605–608.

Klinkenberg, M., Thurow, N., Gispert, S., Ricciardi, F., Eich, F., Prehn, J.H., Auburger, G., and Kögel, D. (2010). Enhanced vulnerability of PARK6 patient skin fibroblasts to apoptosis induced by proteasomal stress. Neuroscience 166, 422–434.

Kondapalli, C., Kazlauskaite, A., Zhang, N., Woodroof, H.I., Campbell, D.G., Gourlay, R., Burchell, L., Walden, H., Macartney, T.J., Deak, M., et al. (2012). PINK1 is activated by mitochondrial membrane potential depolarization and stimulates Parkin E3 ligase activity by phosphorylating Serine 65. Open Biol. 2, 120080.

Kornberg, A., Lieberman, I., and Simms, E.S. (1955). Enzymatic synthesis of purine nucleotides. J. Biol. Chem. 215, 417–427.

Krishnan, P., Fu, Q., Lam, W., Liou, J.Y., Dutschman, G., and Cheng, Y.C. (2002). Phosphorylation of pyrimidine deoxynucleoside analog diphosphates: selective phosphorylation of L-nucleoside analog diphosphates by 3-phosphoglycerate kinase. J. Biol. Chem. 277, 5453–5459.

Kulkarni, R.N., Brüning, J.C., Winnay, J.N., Postic, C., Magnuson, M.A., and Kahn, C.R. (1999). Tissue-specific knockout of the insulin receptor in pancreatic beta cells creates an insulin secretory defect similar to that in type 2 diabetes. Cell 96, 329–339.

Lang, A.E., and Lozano, A.M. (1998). Parkinson's disease. First of two parts. N. Engl. J. Med. 339, 1044–1053.

Lieberman, I., Kornberg, A., and Simms, E.S. (1955a). Enzymatic synthesis of nucleoside diphosphates and triphosphates. J. Biol. Chem. 215, 429–440.

Lieberman, I., Kornberg, A., and Simms, E.S. (1955b). Enzymatic synthesis of pyrimidine nucleotides; orotidine-5′-phosphate and uridine-5′-phosphate. J. Biol. Chem. 215, 403–451.

Liu, Y., Shah, K., Yang, F., Witucki, L., and Shokat, K.M. (1998a). A molecular gate which controls unnatural ATP analogue recognition by the tyrosine kinase v-Src. Bioorg. Med. Chem. 6, 1219–1226.

Meissner, C., Lorenz, H., Weihofen, A., Selkoe, D.J., and Lemberg, M.K. (2011). The mitochondrial intramembrane protease PARL cleaves human Pink1 to regulate Pink1 trafficking. J. Neurochem. *117*, 856–867.

Merrick, K.A., Wohlbold, L., Zhang, C., Allen, J.J., Horiuchi, D., Huskey, N.E., Goga, A., Shokat, K.M., and Fisher, R.P. (2011). Switching Cdk2 on or off with small molecules to reveal requirements in human cell proliferation. Mol. Cell *42*, 624–636.

Mills, R.D., Sim, C.H., Mok, S.S., Mulhern, T.D., Culvenor, J.G., and Cheng, H.C. (2008). Biochemical aspects of the neuroprotective mechanism of PTEN-induced kinase-1 (PINK1). J. Neurochem. *105*, 18–33.

Nakamura, K., Nemani, V.M., Azarbal, F., Skibinski, G., Levy, J.M., Egami, K., Munishkina, L., Zhang, J., Gardner, B., Wakabayashi, J., et al. (2011). Direct membrane association drives mitochondrial fission by the Parkinson disease-associated protein alpha-synuclein. J. Biol. Chem. *286*, 20710–20726.

Narendra, D., Tanaka, A., Suen, D.F., and Youle, R.J. (2008). Parkin is recruited selectively to impaired mitochondria and promotes their autophagy. J. Cell Biol. *183*, 795–803.

Narendra, D.P., Jin, S.M., Tanaka, A., Suen, D.-F., Gautier, C.A., Shen, J., Cookson, M.R., and Youle, R.J. (2010). PINK1 is selectively stabilized on impaired mitochondria to activate Parkin. PLoS Biol. *8*, e1000298.

Niefind, K., Pütter, M., Guerra, B., Issinger, O.G., and Schomburg, D. (1999). GTP plus water mimic ATP in the active site of protein kinase CK2. Nat. Struct. Biol. *6*, 1100–1103.

Nishizuka, Y. (1984). The role of protein kinase C in cell surface signal transduction and tumour promotion. Nature *308*, 693–698.

Nunnari, J., and Suomalainen, A. (2012). Mitochondria: in sickness and in health. Cell *148*, 1145–1159.

Parkin, D.W., Leung, H.B., and Schramm, V.L. (1984). Synthesis of nucleotides with specific radiolabels in ribose. Primary 14C and secondary 3H kinetic isotope effects on acid-catalyzed glycosidic bond hydrolysis of AMP, dAMP, and inosine. J. Biol. Chem. *259*, 9411–9417.

Petit, A., Kawarai, T., Paitel, E., Sanjo, N., Maj, M., Scheid, M., Chen, F., Gu, Y., Hasegawa, H., Salehi-Rad, S., et al. (2005). Wild-type PINK1 prevents basal and induced neuronal apoptosis, a protective effect abrogated by Parkinson disease-related mutations. J. Biol. Chem. *280*, 34025–34032.

Pridgeon, J.W., Olzmann, J.A., Chin, L.S., and Li, L. (2007). PINK1 protects against oxidative stress by phosphorylating mitochondrial chaperone TRAP1. PLoS Biol. *5*, e172.

Qiao, Y., Molina, H., Pandey, A., Zhang, J., and Cole, P.A. (2006). Chemical rescue of a mutant enzyme in living cells. Science *311*, 1293–1297.

Ray, A.S., Vela, J.E., Olson, L., and Fridland, A. (2004). Effective metabolism and long intracellular half life of the anti-hepatitis B agent adefovir in hepatic cells. Biochem. Pharmacol. *68*, 1825–1831.

Rugarli, E.I., and Langer, T. (2012). Mitochondrial quality control: a matter of life and death for neurons. EMBO J. *31*, 1336–1349.

Samaranch, L., Lorenzo-Betancor, O., Arbelo, J.M., Ferrer, I., Lorenzo, E., Irigoyen, J., Pastor, M.A., Marrero, C., Isla, C., Herrera-Henriquez, J., and Pastor, P. (2010). PINK1-linked parkinsonism is associated with Lewy body pathology. Brain *133*, 1128–1142.

Shah, K., Liu, Y., Deirmengian, C., and Shokat, K.M. (1997). Engineering unnatural nucleotide specificity for Rous sarcoma virus tyrosine kinase to uniquely label its direct substrates. Proc. Natl. Acad. Sci. USA *94*, 3565–3570.

Shetty, R.S., Gallagher, C.S., Chen, Y.T., Hims, M.M., Mull, J., Leyne, M., Pickel, J., Kwok, D., and Slaugenhaupt, S.A. (2011). Specific correction of a splice defect in brain by nutritional supplementation. Hum. Mol. Genet. *20*, 4093–4101.

Shin, J.H., Ko, H.S., Kang, H., Lee, Y., Lee, Y.I., Pletinkova, O., Troconso, J.C., Dawson, V.L., and Dawson, T.M. (2011). PARIS (ZNF746) repression of PGC-1α contributes to neurodegeneration in Parkinson's disease. Cell *144*, 689–702.

Song, S., Jang, S., Park, J., Bang, S., Choi, S., Kwon, K.Y., Zhuang, X., Kim, E., and Chung, J. (2013). Characterization of phosphatase and tensin homolog (PTEN)-induced putative kinase 1 (PINK1) mutations associated with Parkinson's disease in mammalian cells and Drosophila. J. Biol. Chem. *288*, 5660–5672.

Ultanir, S.K., Hertz, N.T., Li, G., Ge, W.P., Burlingame, A.L., Pleasure, S.J., Shokat, K.M., Jan, L.Y., and Jan, Y.N. (2012). Chemical genetic identification of NDR1/2 kinase substrates AAK1 and Rabin8 Uncovers their roles in dendrite arborization and spine development. Neuron *73*, 1127–1142.

Valente, E.M., Abou-Sleiman, P.M., Caputo, V., Muqit, M.M., Harvey, K., Gispert, S., Ali, Z., Del Turco, D., Bentivoglio, A.R., Healy, D.G., et al. (2004). Hereditary early-onset Parkinson's disease caused by mutations in PINK1. Science *304*, 1158–1160.

Vela, J.E., Olson, L.Y., Huang, A., Fridland, A., and Ray, A.S. (2007). Simultaneous quantitation of the nucleotide analog adefovir, its phosphorylated anabolites and 2′-deoxyadenosine triphosphate by ion-pairing LC/MS/MS. J. Chromatogr. B Analyt. Technol. Biomed. Life Sci. *848*, 335–343.

Wang, H.L., Chou, A.H., Yeh, T.H., Li, A.H., Chen, Y.L., Kuo, Y.L., Tsai, S.R., and Yu, S.T. (2007). PINK1 mutants associated with recessive Parkinson's disease are defective in inhibiting mitochondrial release of cytochrome c. Neurobiol. Dis. *28*, 216–226.

Wang, X., Winter, D., Ashrafi, G., Schlehe, J., Wong, Y.L., Selkoe, D., Rice, S., Steen, J., LaVoie, M.J., and Schwarz, T.L. (2011). PINK1 and Parkin target Miro for phosphorylation and degradation to arrest mitochondrial motility. Cell *147*, 893–906.

Wei, L., Gao, X., Warne, R., Hao, X., Bussiere, D., Gu, X.J., Uno, T., and Liu, Y. (2010). Design and synthesis of benzoazepin-2-one analogs as allosteric binders targeting the PIF pocket of PDK1. Bioorg. Med. Chem. Lett. *20*, 3897–3902.

Xiong, H., Wang, D., Chen, L., Choo, Y.S., Ma, H., Tang, C., Xia, K., Jiang, W., Ronai, Z., Zhuang, X., and Zhang, Z. (2009). Parkin, PINK1, and DJ-1 form a ubiquitin E3 ligase complex promoting unfolded protein degradation. J. Clin. Invest. *119*, 650–660.

Youle, R.J., and Narendra, D.P. (2011). Mechanisms of mitophagy. Nat. Rev. Mol. Cell Biol. *12*, 9–14.

Zhou, Z.R., Zhang, Y.H., Liu, S., Song, A.X., and Hu, H.Y. (2012). Length of the active-site crossover loop defines the substrate specificity of ubiquitin C-terminal hydrolases for ubiquitin chains. Biochem. J. *441*, 143–149.

EXTENDED EXPERIMENTAL PROCEDURES

Identification of PINK1 Autophosphorylation Site by Liquid Chromatography-Tandem Mass Spectrometry

PINK1[WT] and PINK1[KDDD] were incubated with KTPγS in the presence of cell lysate, digested with trypsin, and thiophosphorylated peptides were captured using established methods as described (Ultanir et al., 2012). Captured peptides were analyzed by liquid chromatography-tandem mass spectrometry (LC/MS/MS) analysis on a Velos Orbitrap (Thermo). PINK1 autophosphorylation site was found only with PINK1[WT] and KTPγS which indicates this nucleotide is utilized as a bona fide substrate.

Details for Enzymatic Production of KMP In Vitro

0.5 mM adenine, kinetin or 9MK were added to a solution of 100 mM Tris-HCl pH 7.5, 10 mM MgCl$_2$, 2 mM PRPP (Sigma), and mixed well. Reaction was initiated by addition of 10 U of APRT (Genway Biotech) and the reaction was incubated at 37°C for the indicated time. The reaction was quenched by dilution of the reaction into an equal volume of 0.1% TFA in H$_2$O with 50 mM EDTA at 4°C followed by analysis on an Acquity UPLCMS system (Waters). Production of AMP and KMP were quantified by extracted ion spectrum and peak integration.

Details on HPLC Analysis for KTP Production in Cells

HeLa cells were grown in DMEM supplemented with 10% FBS with either 0.05% DMSO or 25 μM Kinetin for 96 hr. For each assay six 15-cm plates of confluent HeLa cells were washed with ice cold PBS, scraped into 5 ml ice cold PBS pelleted and lysed by addition of a volume of 80% Methanol at −80°C equal to the cell pellet for lysis and deproteination. Cells were vigorously resuspended on ice and left for 2 hr at −20°C before vortexing for 10 s and centrifugation at top speed. The pellet was then washed with 1 pellet volume of ice cold water and this was added to the lysate along with an appropriate volume of 10 mM BTP to 250 μM final. 20 μl was then injected onto a HPLC (Waters) and analyzed by a linear gradient from 100% buffer A (5 mM tetrabutylammonium hydroxide (TBAH) 25 mM KH$_2$PO$_4$ 5% acetonitrile) to 65% buffer B (5 mM tetrabutylammonium hydroxide (TBAH) 25 mM KH$_2$PO$_4$ 60% acetonitrile) over 37.5 min. Concentration of ATP, KTP and other nucleotides were determined by comparing to a standard dilution curve of each.

Details on Automated Quantitation of Parkin Mitochondrial Translocatin

To calculate the fraction of Parkin recruited to mitochondria, a cell mask was determined for each cell by manually drawing the cell boundary and a mitochondrial mask was determined by thresholding the GFP channel using Otsu's method (Otsu, 1979). The fraction of Parkin recruited to mitochondria was then calculated as the total mCherry intensity within the mitochondrial mask divided by the total mCherry intensity within the cell mask. Delta co-localization was calculated by subtracting the fraction of Parkin recruited to mitochondria at t = 0 from each subsequent time point. Cells with poor mCherry expression were excluded by requiring a minimum total mCherry signal within the cell mask.

Dopamine Neuron Cultures

Midbrain neuronal cultures were prepared from early postnatal (P0-P1) rats as described (Nemani et al., 2010). On day 2, cells were treated with kinetin, adenine, 9-methylkinetin or equivalent DMSO (15 μM or 50 μM). On day 14, cells were fixed with 4% paraformaldehyde, and stained against tyrosine hydroxylase (rabbit, Pel-Freez Biologicals) to identify dopamine neurons, and NeuN (mouse, Millipore) to identify total neurons.

PINK1 shRNA Production

PINK1 shRNA lentivirus were produced using a pLKO.1 based shRNA (Sigma) by co-transfection of a 6 cm dish of HEK293T cells with pLKO.1 shRNA vector, Δ8.9 and pMGD2 vectors in a 2:3:1 ratio (3 μg total DNA with 7 μl Fugene 6 in 200 μl of Optimem) and following standard protocols to isolate infective lentivirus particles. HeLa and SH-SY5Y cells were infected with lentivirus followed by selection with puromycin at 10 μg/ml and 1 μg/ml respectively.
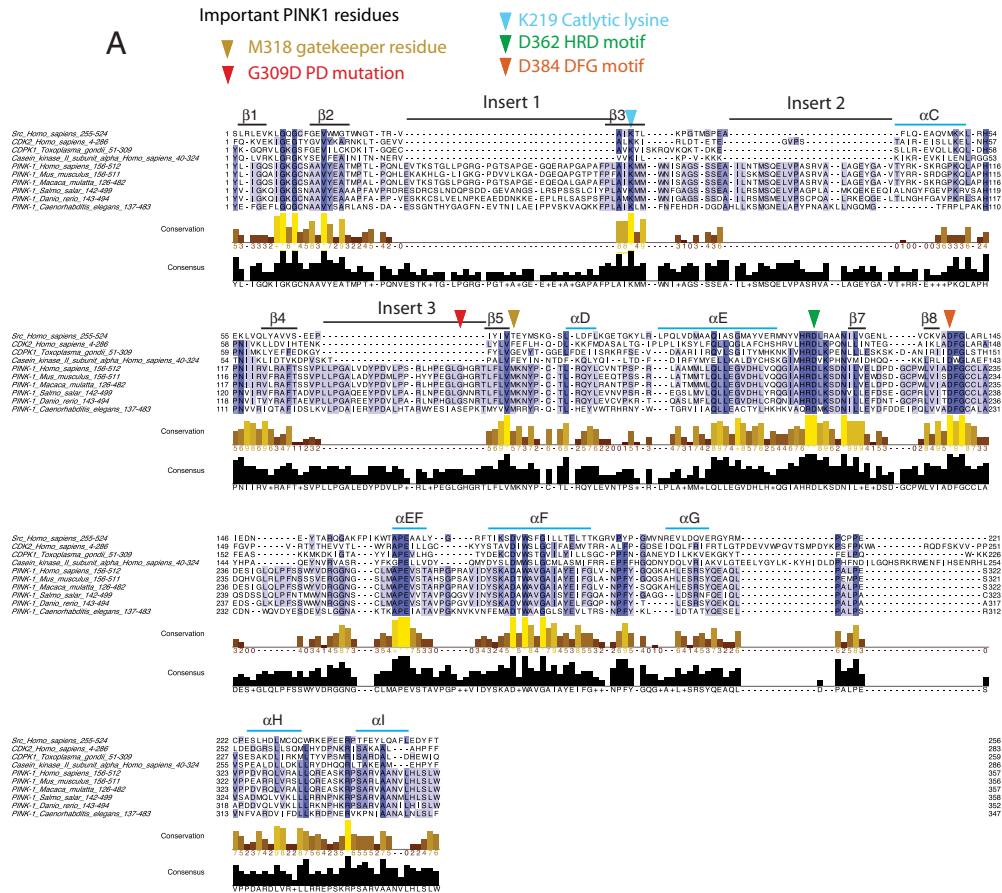
Apoptosis Assays and Phospho-S62 Bcl-xL Immunoblot Analysis

HeLa cells were plated on 96 well assay plates at around 4,000 cells per well and transfected with Parkin in a similar way as in recruitment assays followed by treatment with 25 μM of the indicated drug for 48 hr. Growth medium was then replaced with fresh medium plus 25 μM drug and 1 μM MG132 for 12 hr, followed by addition of one time medium volume Caspase-Glo reagent (Promega), incubated at room temperature in the dark for 1 hr and read on a microplate reader (Molecular Devices) for luminescence.

  SH-SY5Y cells (ATCC) were cultured in 1:1 mix of F12K and DMEM supplemented with 20% FBS. The indicated SH-SY5Y cells were plated in 6-well plates at about 500,000 cells/well, pretreated with 50 μM of the indicated drug or DMSO for 96 hr followed by 400 μM H$_2$O$_2$ treatment. Subsequently, cells were stained with Annexin V-FITC and PI and analyzed (FACS Diva) on a FACS LSRII Cytometer (Beckman Coulter) Apoptosis was calculated as the difference between H$_2$O$_2$ treated samples and the respective control. SH-SY5Y cells pre-treated in the same way followed by 50 μM CCCP treatment for 12 hr were lysed and analyzed for phospho-S62 Bcl-xL (Santa Cruz Biotech), total Bcl-xL, PINK1 and β-actin (all Cell Signaling) by immunoblots.

SUPPLEMENTAL REFERENCES

Banko, M.R., Allen, J.J., Schaffer, B.E., Wilker, E.W., Tsou, P., White, J.L., Villén, J., Wang, B., Kim, S.R., Sakamoto, K., et al. (2011). Chemical genetic screen for AMPKα2 substrates uncovers a network of proteins involved in mitosis. Mol. Cell *44*, 878–892.

Blethrow, J., Zhang, C., Shokat, K.M., and Weiss, E.L. (2004). Design and use of analog-sensitive protein kinases. Curr. Protoc. Mol. Biol. *66*, 18.11.1–18.11.19.

Cibrián Uhalte, E., Kirchner, M., Hellwig, N., Allen, J.J., Donat, S., Shokat, K.M., Selbach, M., and Abdelilah-Seyfried, S. (2012). In vivo conditions to identify Prkci phosphorylation targets using the analog-sensitive kinase method in zebrafish. PLoS ONE *7*, e40000.

Hengeveld, R.C., Hertz, N.T., Vromans, M.J., Zhang, C., Burlingame, A.L., Shokat, K.M., and Lens, S.M. (2012). Development of a chemical genetic approach for human aurora B kinase identifies novel substrates of the chromosomal passenger complex. Mol. Cell. Proteomics *11*, 47–59.

Kaasik, K., Kivimäe, S., Allen, J.J., Chalkley, R.J., Huang, Y., Baer, K., Kissel, H., Burlingame, A.L., Shokat, K.M., Ptáček, L.J., and Fu, Y.H. (2013). Glucose sensor O-GlcNAcylation coordinates with phosphorylation to regulate circadian clock. Cell Metab. *17*, 291–302.

Liu, Y., Shah, K., Yang, F., Witucki, L., and Shokat, K.M. (1998b). Engineering Src family protein kinases with unnatural nucleotide specificity. Chem. Biol. *5*, 91–101.

Lourido, S., Shuman, J., Zhang, C., Shokat, K.M., Hui, R., and Sibley, L.D. (2010). Calcium-dependent protein kinase 1 is an essential regulator of exocytosis in Toxoplasma. Nature *465*, 359–362.

Nemani, V.M., Lu, W., Berge, V., Nakamura, K., Onoa, B., Lee, M.K., Chaudhry, F.A., Nicoll, R.A., and Edwards, R.H. (2010). Increased expression of alpha-synuclein reduces neurotransmitter release by inhibiting synaptic vesicle reclustering after endocytosis. Neuron *65*, 66–79.

Otsu, N. (1979). A threshold selection method from gray-level histograms. IEEE Trans. Syst., Man Cybernetics *SMC-9*, 62–66.

Schauble, S., King, C.C., Darshi, M., Koller, A., Shah, K., and Taylor, S.S. (2007). Identification of ChChd3 as a novel substrate of the cAMP-dependent protein kinase (PKA) using an analog-sensitive catalytic subunit. J. Biol. Chem. *282*, 14952–14959.

Sicheri, F., and Kuriyan, J. (1997). Structures of Src-family tyrosine kinases. Curr. Opin. Struct. Biol. *7*, 777–785.

Tamgüney, T., Zhang, C., Fiedler, D., Shokat, K., and Stokoe, D. (2008). Analysis of 3-phosphoinositide-dependent kinase-1 signaling and function in ES cells. Exp. Cell Res. *314*, 2299–2312.

A

Important PINK1 residues

▼ M318 gatekeeper residue
▼ G309D PD mutation
▼ K219 Catlytic lysine
▼ D362 HRD motif
▼ D384 DFG motif

Insert 1   Insert 2   αC

β1   β2   β3

Src_Homo_sapiens_255-524
CDK2_Homo_sapiens_4-286
CDPK1_Toxoplasma_gondii_51-309
Casein_kinase_II_subunit_alpha_Homo_sapiens_40-324
PINK-1_Homo_sapiens_156-512
PINK-1_Mus_musculus_156-511
PINK-1_Macaca_mulatta_126-482
PINK-1_Salmo_salar_142-499
PINK-1_Danio_rerio_143-494
PINK-1_Caenorhabditis_elegans_137-483

Conservation

Consensus

β4   Insert 3   β5   αD   αE   β7   β8

Conservation

Consensus

αEF   αF   αG

Conservation

Consensus

αH   αI

Conservation

Consensus

B

	Accept N⁶ modified ATP analog?			
kinase	wt-kinase	as-kinase	Gatekeeper (Suppressive)	Reference
PINK1	Yes	NA	NA	NA
Fyn	No	Yes	T339G	Liu, 1998a
vSrc	No	Yes	I338G	Shah, 1997
PKCδ	No	Yes	M425A	Allen, 2007
CDC5	No	Yes	L158G	Allen, 2007
JNK1	No	Yes	M108G(L168A)	Allen, 2007
ERK2	No	Yes	Q103G	Allen, 2007
PKA	No	Yes	M120G	Koller, 2007
PDK1	No	Yes	L159G	Tamgüney, 2008
CDK1	No	Yes	F80G	Blethrow, 2008
AMPKα2	No	Yes	M93G	Banko, 2011
AuroraB	No	Yes	L145G(H250Y)	Hengevold, 2012
NDR1/2	No	Yes	M166A(M152L,S229A)	Ultanir, 2012
αPKC	No	Yes	I613A	Cibrián Uhalte, 2012
GSK3β	No	Yes	L132A	Kaasik, 2013

Figure S1. Alignment of PINK1 to Typical and Atypical Kinase Domains Reveals Several Large Inserts in the N Lobe of PINK1, Related to Figure 1

(A) T-coffee alignment of PINK1 (*Homo sapiens*, *Mus musculus*, macaca mulatta, salmo salar, danio rerio, *Caenorhabditis elegans*) to *Homo sapiens* Src (secondary structure based on the Src structure shown [Sicheri and Kuriyan, 1997]) and CDK1 reveals a larger residue in the gatekeeper position (gold triangle) of these two kinases that do not accept N6 modified "bumped" ATP analogs (Liu et al., 1998a; Merrick et al., 2011). However, in CDPK, a gatekeeper glycine provides space for "bumped" ATP competitive kinase inhibitors (Lourido et al., 2010). The alignment reveals 3 large inserts in the N-lobe of PINK1, including an insert directly before the predicted gatekeeper residue containing the location of glycine 309 whose mutation leads to a loss of kinase activity. Three catalytic residues (catalytic lysine, D in the HRDL and D in the DFG motif) are conserved across all kinases.

(B) Comparison of kinases in which the activity with ATP and N6 modified ATP has been studied. These 14 previously published kinases have all been analyzed for the ability to utilize N6 modified ATP analogs before and after mutation of the gatekeeper residue (Allen et al., 2007; Banko et al., 2011; Blethrow et al., 2008; Cibrián Uhalte et al., 2012; Hengeveld et al., 2012; Kaasik et al., 2013; Liu et al., 1998a, 1998b; Schauble et al., 2007; Shah et al., 1997; Tamgüney et al., 2008; Ultanir et al., 2012).
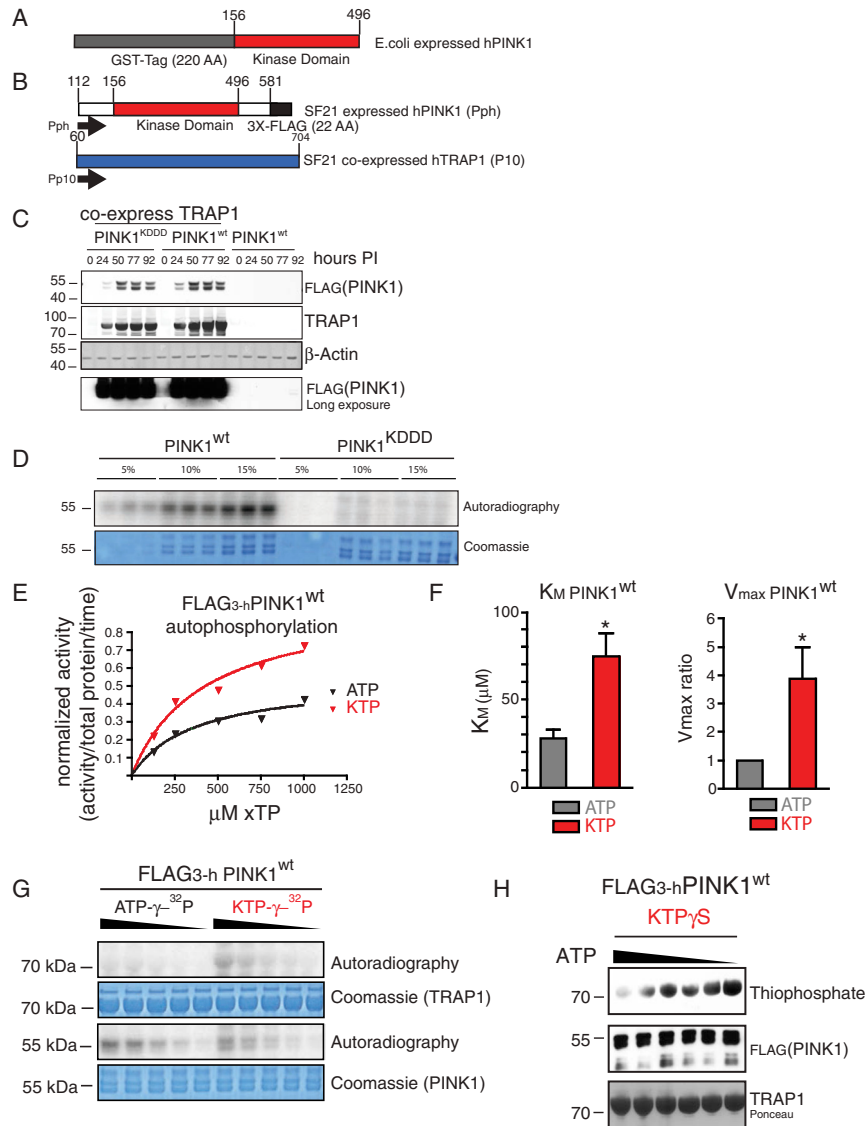
Figure S2. Optimized PINK1 Expression Constructs Used to Express PINK1 for Enzymatic Characterization, Related to Figure 1

(A) GST tagged PINK1 kinase domain (156-496) expressed in bacteria.

(B) Schematic depicting the expression construct for PINK1 kinase domain (112-581) co-expression with TRAP1 in insect cells. PINK1 is driven by the Pph promoter and TRAP1 is driven by the Pp10 promoter.

(C) SF21 infected insect cells were lysed and analyzed by immunoblotting for FLAG PINK1, TRAP1 and β-actin. TRAP1 expression leads to higher amounts of PINK1 expression.

(D) Baculovirus produced PINK1^{KDDD} has severely compromised kinase activity with γ^{32}P ATP, whereas PINK1^{WT} shows robust autophosphorylation activity.

(E and F) PINK1^{WT} was incubated with either ATPγS or KTPγS at the indicated concentration. Activity was assessed by Western blot for thiophospho-PINK1, subtracting t_0 background thiophosphate signal and normalizing to total PINK1 signal. Velocity was plotted (a representative experiment shown) and the V_{max} and K_M for each nucleotide was calculated. K_M for ATPγS and KTPγS (27.9 $\pm$ 4.9 μM; 74.6 $\pm$ 13.2 μM) (mean $\pm$ SEM; p = 0.02;t test). V_{max} was plotted as the ratio of KTPγS /ATPγS (3.9 $\pm$ 1.3 fold higher (p = 0.02;t test).

(G) Kinetin γ^{32}P ATP was generated using a NDPK-ATP coupled system (Blethrow et al., 2004). PINK1^{WT} was incubated with either radiolabeled ATP or KTP along with substrate TRAP1. PINK1^{WT} phosphorylates TRAP1 with higher activity utilizing KTP-γ^{32}P than ATP-γ^{32}P, and autophosphorylates with both nucleotides.

(H) PINK1^{WT} was incubated with substrate $_{60-704}$TRAP1 (74 kDa at 1 mg/ml) and 500 μM nucleotide KTPγS along with varying amounts of competing non-thiophosphorylated ATP (from 2 mM to 62.5 μM to in 1:2 dilution series). PINK1 activity was analyzed by Western blotting for thiophospho-labeled protein. PINK1 utilized KTPγS, visualized by thiophosphorylation, with up to an 8 fold excess of ATP (lane 1).
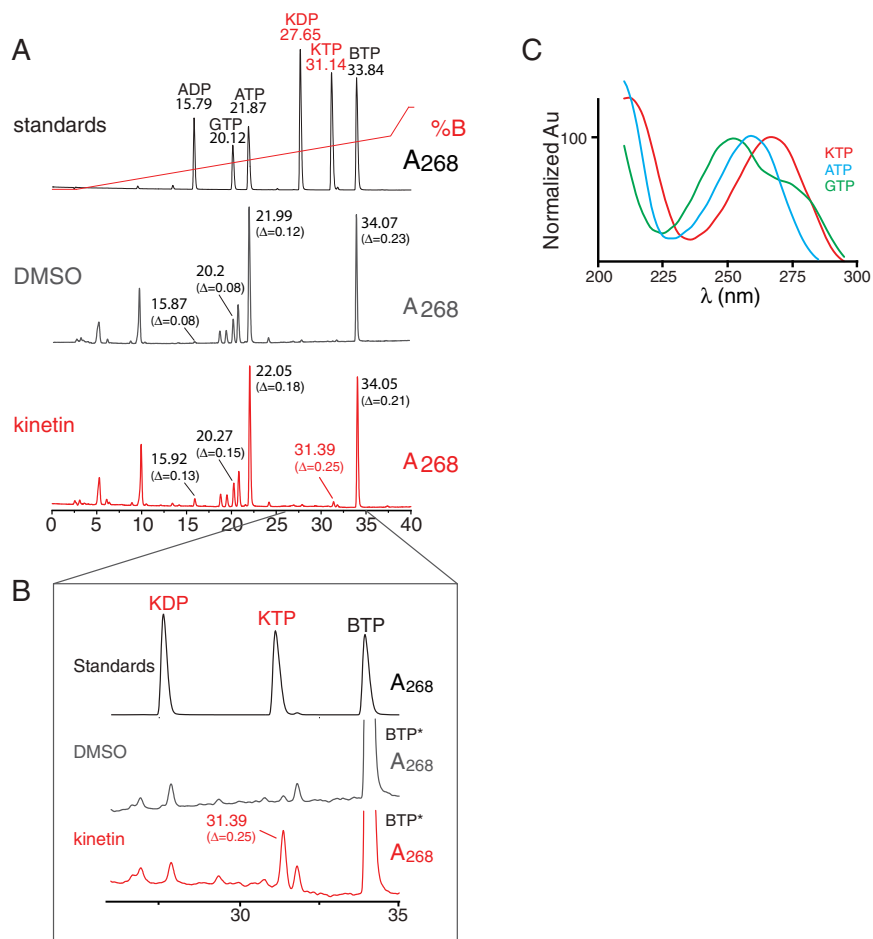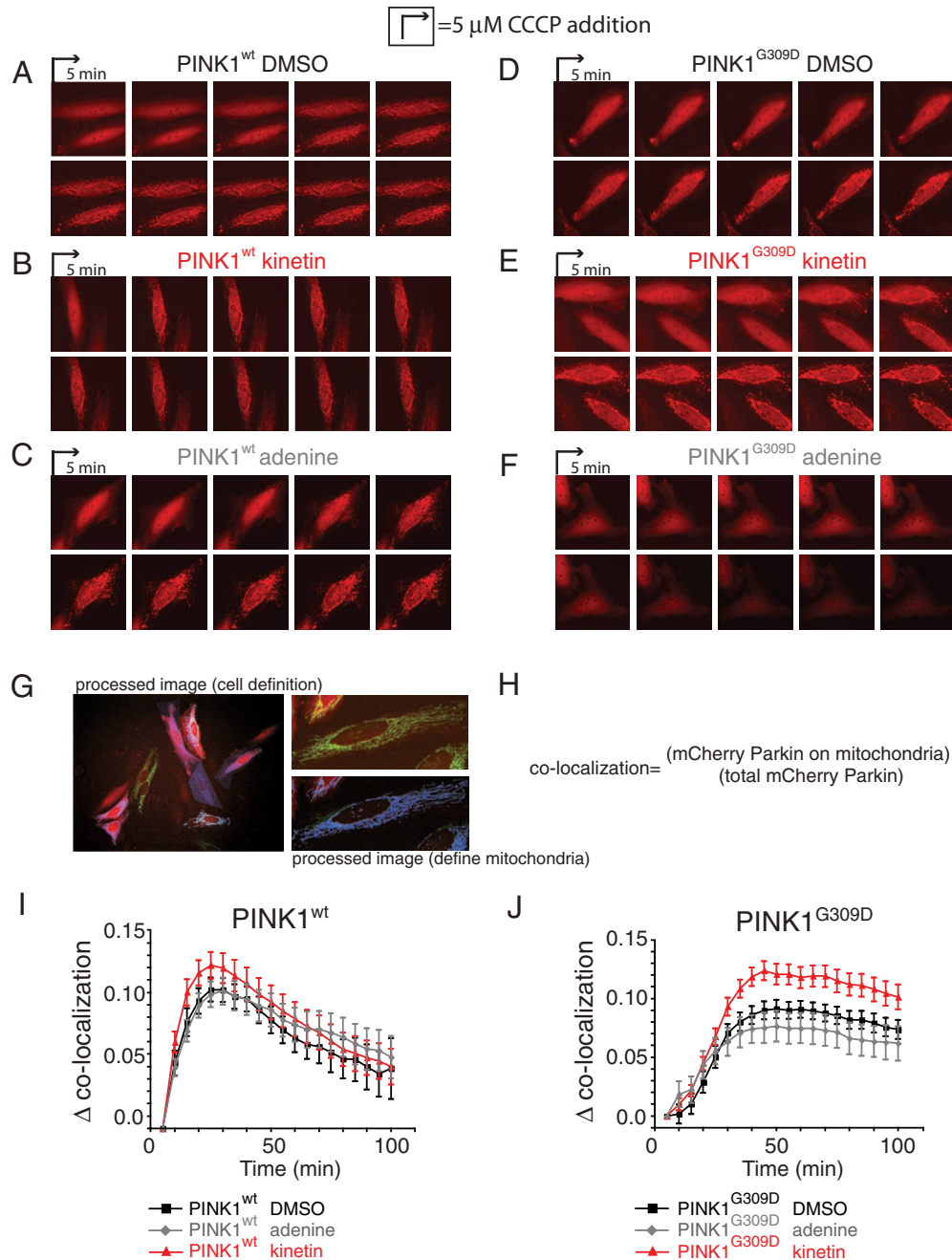
Figure S3. Neo-Substrate Precursor Kinetin Leads to KTP in Human Cells, Related to Figure 2 and Table 1

(A) HPLC analysis of 20 μl of either 0.5 mM standards (ADP, GTP, ATP, KDP, KTP, BTP) or cellular lysate of DMSO or kinetin treated HeLa cells with 250 μM BTP* addition reveals a novel peak present in kinetin treated cells at 31.39 min. The retention time of each peak in the cell lysate was offset, that difference is shown here.

(B) Zoom in of the region from 22.5 to 35 min of the HPLC traces shown in A and in Figure 2D.

(C) Absorbance spectrum of the standards GTP, ATP and KTP.

Figure S4. Addition of Neo-Substrate Precursor Kinetin to HeLa Cells Leads to Increased Parkin Recruitment to Depolarized Mitochondria in a PINK1-Dependent Manner, Related to Figure 3 and Table 2

(A–F) Sequential images of HeLa cells expressing mCherryParkin, mitoGFP and PINK1[WT] (A-C) or PINK1[G309D] (D-F) following CCCP induced depolarization.

(G) A cell mask was determined for each cell by manually drawing the cell boundary and a mitochondrial mask was determined, depicted in the lower right panel.

(H) Equation used to calculate the extent of colocalization (see also Data S1).

(I and J) HeLa cells meeting a threshold of Parkin expression were quantitated using our co-localization algorithm to identify mitochondria (mitoGFP) and calculate the amount of mCherryParkin on mitochondria. Two-way ANOVA analysis revealed that kinetin has an effect in both cases when compared to adenine (WT; F = 43.65 p < 0.0001, G309D; F = 84.02, p < 0.0001) and DMSO (WT; F = 29.65 p < 0.0001, G309D; F = 85.88, p < 0.0001) (See also Figure S6D) at least 40 cells/experiment n = 3 experiments. All values shown are mean ± SEM.
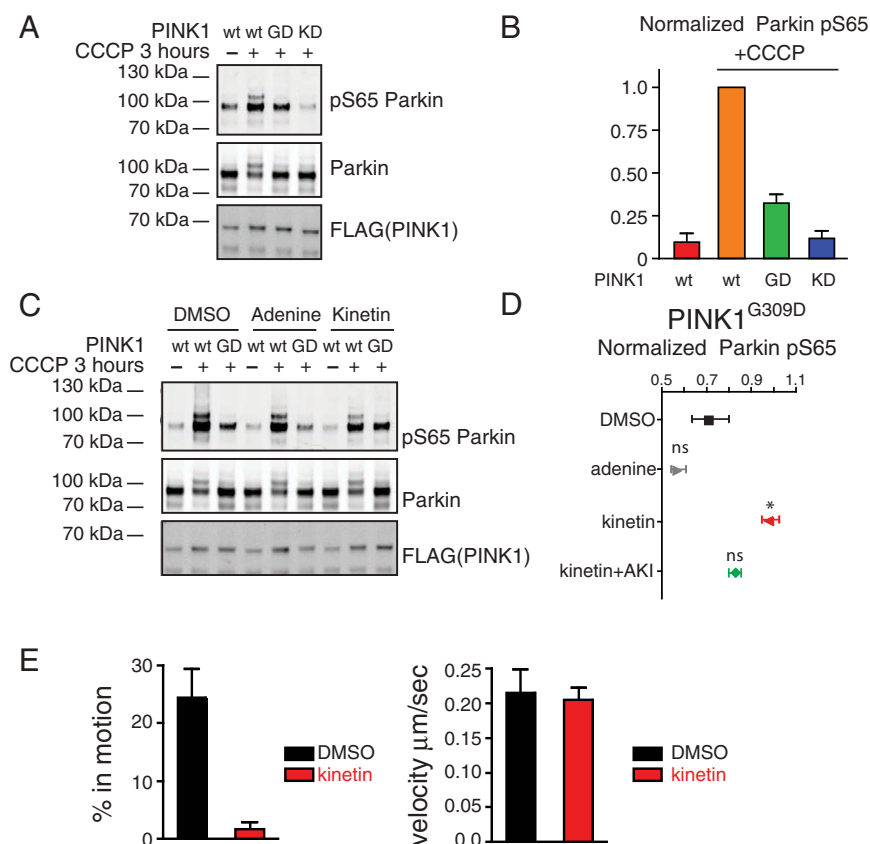
Figure S5. Quantitation of PINK1-Mediated Parkin Phosphorylation at Serine 65 and DMSO Control for Mitochondrial Motility, Related to Figures 3 and 4

(A and B) HeLa cells were transfected with mCherryParkin and either PINK1[WT], PINK1[G309D] or PINK1[KDDD] for 24 hr. Following incubation with CCCP for three hours cells were lysed, mCherryParkin was immunoprecipitated and analyzed by immunoblotting with Parkin S65 phospho-specific antibodies.

(C and D) HeLa cells were transfected with mCherryParkin and either PINK1[WT] or PINK1[G309D] for 24 hr, then incubated with 50 μM adenine, kinetin, kinetin plus 10 nM adenosine kinase inhibitor or equivalent DMSO for 48 hr. mCherryParkin was immunoprecipitated and analyzed by immunoblotting with Parkin S65 phospho-specific antibodies. Normalized Parkin phosphorylation was calculated by normalizing phospho-S65 Parkin signal by total Parkin levels, normalized to phospho-Parkin in untreated cells expressing PINK1[WT] treated with CCCP for three hours.

(E) In C57Bl/6 control mouse hippocampal neuron cultures, kinetin markedly decreases the percentage of moving mitochondria in axons when compared with DMSO control (kinetin DMSO, p < 0.0004). In contrast, kinetin has no effect on the velocity of mitochondrial movement (kinetin DMSO, p = 0.88 (all values are mean ± SEM, two tailed students t test).
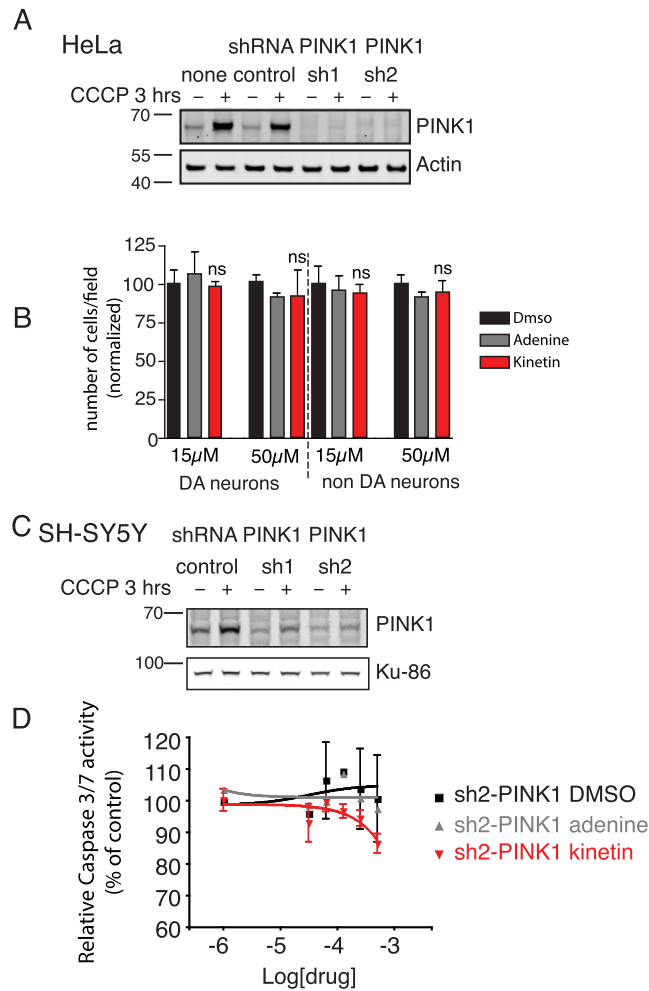
Figure S6. Kinetin Is Nontoxic in Cultured Neurons and Does Not Affect Caspase 3/7 Cleavage Activity in PINK1 shRNA Expressing SH-SY5Y Cells, Related to Figure 5

(A) HeLa cells were infected with a lentivirus (pLKO.1 based vector) expressing either non-mammalian shRNA (sh-control) or one of two (sh1 and sh2) PINK1 directed shRNA constructs. Cells were plated in a six well plates and the indicated lanes depict cells treated with 10 μM CCCP for 3 hr. Following CCCP treatment cells were lysed and analyzed by immunoblotting for PINK1 (cell signaling) and a loading control.

(B) Postnatal dopamine neurons were cultured with 50 μM drug for 10 or 12 days (days 2-14). The mean number of surviving dopamine and non-dopamine neurons per field was quantified.

(C) SH-SY5Y cells were treated with lentivirus as in (A).

(D) SH-SY5Y cells were pre-treated with varying concentration of adenine or kinetin (constant DMSO) for 96 hr followed by concurrent 1 μM MG132 treatment for 12 hr in all conditions. Caspase 3/7 cleavage activity was quantified as in Figures 5A and 5B, with the comparison made to the DMSO only control. Two-way ANOVA analysis revealed that kinetin has no effect when compared to DMSO or adenine (DMSO; F = 3.552 p = 0.084;adenine; F = 1.7 p = 0.215) in cells expressing an shRNA against PINK1.

All values are mean ± SEM.